

Geochemistry, Geophysics, Geosystems®

RESEARCH ARTICLE

10.1029/2024GC011499

Special Collection:

A fresh look at the Caribbean plate geosystems

Key Points:

- Tectonic constraints conflict with previously proposed collision and escape models for Paleogene Caribbean reorganization
- Slab reconstructions and geodynamic models suggest Farallon slab anchoring induced tectonic reorganization
- In this model, lower mantle slab penetration triggers mantle flow, lithospheric compression, and subduction initiation

Supporting Information:

Supporting Information may be found in the online version of this article.

Correspondence to:

E. M. Conrad,
econrad@utexas.edu

Citation:

Conrad, E. M., Faccenna, C., Holt, A. F., & Becker, T. W. (2024). Tectonic reorganization of the Caribbean plate system in the Paleogene driven by Farallon slab anchoring. *Geochemistry, Geophysics, Geosystems*, 25, e2024GC011499. <https://doi.org/10.1029/2024GC011499>

Received 7 FEB 2024

Accepted 21 JUL 2024

Author Contributions:

Conceptualization: Ethan M. Conrad, Claudio Faccenna, Adam F. Holt, Thorsten W. Becker

Data curation: Ethan M. Conrad, Adam F. Holt

Formal analysis: Ethan M. Conrad, Adam F. Holt

Funding acquisition: Adam F. Holt, Thorsten W. Becker

© 2024 The Author(s). *Geochemistry, Geophysics, Geosystems* published by Wiley Periodicals LLC on behalf of American Geophysical Union.

This is an open access article under the terms of the [Creative Commons](#)

[Attribution License](#), which permits use, distribution and reproduction in any medium, provided the original work is properly cited.

Tectonic Reorganization of the Caribbean Plate System in the Paleogene Driven by Farallon Slab Anchoring



Ethan M. Conrad¹ , Claudio Faccenna^{2,3} , Adam F. Holt⁴ , and Thorsten W. Becker^{1,5} 

¹Institute for Geophysics and Department of Earth and Planetary Sciences, Jackson School of Geosciences, The University of Texas at Austin, Austin, TX, USA, ²Department of Science, Università Roma TRE, Roma, Italy, ³German Research Centre for Geosciences (GFZ), Potsdam, Germany, ⁴Rosenstiel School of Marine, Atmospheric, and Earth Sciences, University of Miami, Miami, FL, USA, ⁵Oden Institute for Computational Engineering & Sciences, The University of Texas at Austin, Austin, TX, USA

Abstract The tectonic configuration of the Caribbean plate is defined by inward-dipping double subduction at its boundaries with the North American and Cocos plates. This geometry resulted from a Paleogene plate reorganization, which involved the abandonment of an older subduction system, the Great Arc of the Caribbean (GAC), and conversion into a transform margin during Lesser Antilles (LA) arc formation. Previous models suggest that a collision between the GAC and the Bahamas platform along the North American passive margin caused this event. However, geological and geophysical constraints from the Greater Antilles do not show a large-scale compressional episode that should correspond to such a collision. We propose an alternative model for the evolution of the region where lower mantle penetration of the Farallon slab promotes the onset of subduction at the LA. We integrate tectonic constraints with seismic tomography to analyze the timing and dynamics of the reorganization, showing that the onset of LA subduction corresponds to the timing of Farallon/Cocos slab penetration. With numerical subduction models, we explore whether slab penetration constitutes a dynamically feasible set of mechanisms to initiate subduction in the overriding plate. In our models, when the first slab (Farallon/Cocos) enters the lower mantle, compressive stresses increase at the eastern margin of the upper plate, and a second subduction zone (LA) is initiated. The resulting first-order slab geometries, timings, and kinematics compare well with plate reconstructions. More generally, similar slab dynamics may provide a mechanism not only for the Caribbean reorganization but also for other tectonic episodes throughout the Americas.

Plain Language Summary The Caribbean tectonic plate is bounded by subduction to the east and west. However, it is unclear how this plate configuration was achieved. Previous models suggest that the North American continental margin entered an ancient Caribbean subduction zone between 66 and 34 Mya, converting the margin to strike-slip and initiating subduction to the east at the Lesser Antilles. However, the deformation expected for this event is absent at the site of the supposed collision. Considering geological and geophysical constraints across the Caribbean, we instead suggest that mantle processes drove the reorganization. Combining tomographic images of the mantle with plate modeling, we reconstruct subduction below the Caribbean. Then, through numerical mantle convection modeling, we simulate the Caribbean subduction setting at the time of the reorganization. Our results show that when a subducting plate enters the lower, higher viscosity part of the mantle, it affects mantle flow, causing compression in the overriding plate and the potential initiation of a second subduction zone. The timing when the first slab enters the lower mantle and subduction initiates aligns well with our reconstructions and geological constraints in the Caribbean. We hypothesize that a similar process may explain other major deformation episodes throughout the Americas.

1. Introduction

The subduction of the oceanic lithosphere is the main driver of plate motions, and with that, induces mantle flow around the descending slab (e.g., Forsyth & Uyeda, 1975; Hager, 1984; Hager & O'Connell, 1978). In particular, penetration of the slab into the lower mantle can cause a switch from mantle flow that is generally restricted to the upper mantle to larger-scale return flow. Through the traction that this flow exerts on surface plates, this transition can modify trench and upper plate motions, which in turn, affect tectonics, such as by inducing horizontal compression in the upper plate (e.g., Faccenna et al., 2013; Husson et al., 2012; Yamato et al., 2013; Yang et al., 2016; Zhong & Gurnis, 1995).

Investigation: Ethan M. Conrad, Claudio Faccenna, Adam F. Holt

Methodology: Ethan M. Conrad, Claudio Faccenna, Adam F. Holt, Thorsten W. Becker

Resources: Claudio Faccenna

Supervision: Claudio Faccenna, Thorsten W. Becker

Validation: Claudio Faccenna, Adam F. Holt, Thorsten W. Becker

Visualization: Ethan M. Conrad, Claudio Faccenna, Adam F. Holt

Writing – original draft: Ethan M. Conrad, Claudio Faccenna, Adam F. Holt

Writing – review & editing:

Claudio Faccenna, Adam F. Holt, Thorsten W. Becker

One tectonic system that might regionally respond to such slab dynamics is the Caribbean domain (Figure 1), an example of a double subduction setting, where at present the opposing Farallon/Cocos and Lesser Antilles (LA) slabs are inward dipping (i.e., facing each other in a “bidirectional” sense, cf. Holt et al., 2017). This geodynamic framework provides an opportunity to explore the connection between the two subduction systems and their corresponding role in controlling Caribbean tectonics throughout the Cenozoic Era.

Targeting the dynamic conditions surrounding the onset of subduction at the LA, we focus on the Paleogene (66–23 Ma) evolution of the region. During this period, the plate system re-organized, with the eastern boundary transitioning from an older subduction zone, the Great Arc of the Caribbean (GAC), into a transform margin during the formation of the LA arc (e.g., Boschman et al., 2014; Burke, 1988; Pindell & Kennan, 2009). Previous studies explain the Paleogene reorganization from a collision and escape perspective (e.g., Boschman et al., 2014; Burke, 1988; Escalona et al., 2021; Pindell & Kennan, 2009). The Bahamas platform is a carbonate body that overlies a crustal transition from a thin continental crust north of Cuba to a normal oceanic crust north of Puerto Rico (PR) (Shipper & Mann, 2024). The collision of the Bahamas platform with the GAC trench has been suggested to lead to a sudden eastward shift in the absolute motion of the Caribbean plate and reorganization of the plate margins (e.g., Boschman et al., 2014; Mann et al., 1995; Pindell & Kennan, 2009).

Subduction continues north of Hispaniola and PR to the present day (Benford et al., 2012; Calais et al., 2016; Symithe et al., 2015) with blueschist metamorphism continuing until the early Oligocene (Catlos & Sorensen, 2003; Escuder Viruete & Pérez Estaún, 2004; Joyce, 1991). There is also no record of accreted Bahamas platform material observed in Hispaniola, PR, and the Virgin Islands (Mann et al., 1991). Without fully jamming the subduction trench and accreting plateau material, it is unclear how such an event would lead to the large-scale reorganization of the Caribbean plate margins (Cerpa et al., 2021; van Benthem et al., 2014). A protracted collision model is required to explain the delay in deformation in the central and eastern Greater Antilles (late Eocene to Oligocene; e.g., Laó-Dávila, 2014; Mann et al., 1991; Román et al., 2020) after the onset of collision in the late Paleocene to Eocene (e.g., Bralower & Iturralde-Vinent, 1997; Gordon et al., 1997; Meyerhoff & Hatten, 1968; Pardo, 1975). In conjunction with the spreading record in the LA backarc and paleomagnetic record in PR, these arguments have led some authors to question the role of the Bahamas platform in the Paleogene plate reorganization, positing that compression across the Greater Antilles is caused by either the presence of a pre-existing arcuate subduction corner (Cerpa et al., 2021) or a “push” from the edge of the LA slab (van Benthem et al., 2014).

Using geological and geophysical data, and guided by processes observed in new numerical models, we reconstruct a dynamically consistent scenario for the Cenozoic evolution of the Caribbean plate and the origin of the LA arc within the framework of an inward dipping double subduction system. We argue that, similar to orogenesis in South America (Faccenna et al., 2017), the penetration of the Farallon slab may have triggered the Paleogene reorganization event, causing the initiation/reactivation of a new subduction zone and the establishment of the present, dynamically linked double subduction setting. Considering such regional slab interactions is essential to both the problem of subduction initiation/reactivation in the Atlantic and understanding the linkage between deep mantle processes and surface tectonics. The Paleogene reorganization of the Caribbean may be linked to large-scale, progressive slab anchoring with profound effects on other segments of the Farallon subduction margin, and the Bahamas platform may have played a less significant role than previously thought.

2. Caribbean Tectonics During the Cenozoic

The Caribbean plate mainly comprises a thick, slightly deformed oceanic crust formed during two major plume-related volcanic events from 140–110 and 97–70 Ma, respectively (e.g., Whattam, 2018; Whattam & Stern, 2015). Models suggest that the first event intruded the Farallon Plate in the Pacific, away from the subduction margin, and later entered and jammed the trench, causing a polarity reversal and the onset of west-dipping subduction at the GAC. During the later migration of the GAC into the Atlantic (e.g., Boschman et al., 2014), east-dipping subduction was rejuvenated on the western side of the Caribbean plate around 70–90 Ma (Buchs et al., 2010; Pindell & Kennan, 2009). The second volcanic episode completed the construction of the Caribbean Large Igneous Province (CLIP) and may have been the result of a slab window (Pindell et al., 2006) or interactions between the GAC and Farallon slabs (Riel et al., 2023). The modern Caribbean plate is flanked by asymmetric subduction zones to the east (Atlantic) and west (Pacific). On the Pacific side, seismic tomography shows the Farallon/Cocos slab crossing the 660 km discontinuity and penetrating the lower mantle at a roughly

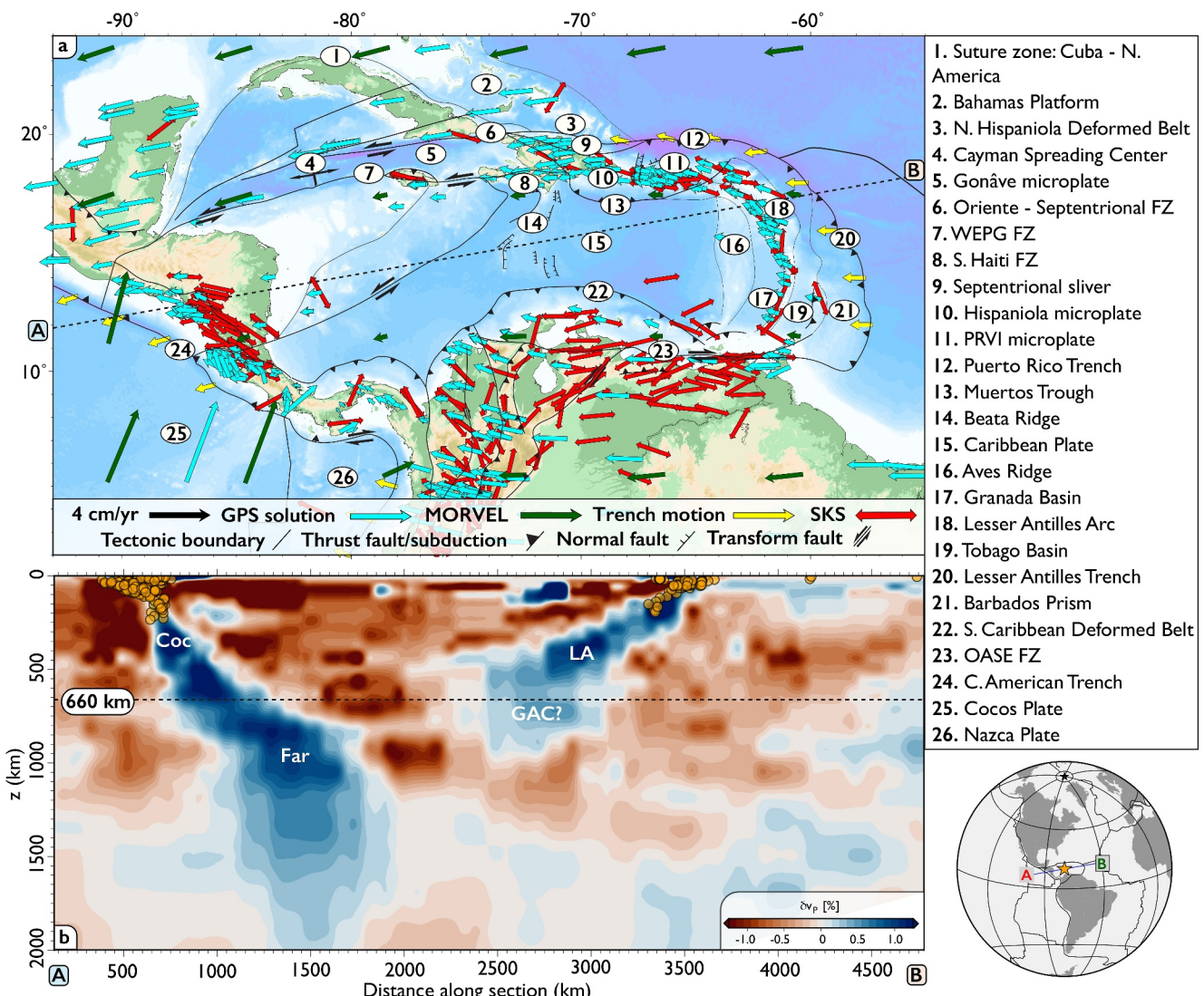


Figure 1. Tectonic setting of the Caribbean. (a) Major tectonic boundaries (black lines, modified after: Boschman et al., 2014; Mann et al., 2002; Pindell & Kennan, 2009), active subduction or major thrust faults (black lines with black triangles), transform faults (black lines with arrows in opposite directions), GPS velocities (cyan arrows; Blewitt et al., 2016), MORVEL plate motions (green arrows; DeMets et al., 2010), trench motion (yellow arrows; Heuret & Lallemand, 2005), and SKS splitting (red double arrows; updated from the compilation of Becker et al., 2012); all velocities in the spreading aligned, absolute reference frame of Becker et al. (2015). WEPG: Walton-Enriquillo-Plantain-Garden. OASE: Oca-Ancón-San Sebastian-El Pilar. (b) Seismic tomography cross section (model UU-P07 of Amaru, 2007) of the Caribbean arc overlain by earthquakes within ± 50 km of the cross-section (Engdahl et al., 1998). White labels associate velocity anomalies with subducted slabs (Coc = Cocos, Far = Farallon, LA = Lesser Antilles, GAC = Great Arc of the Caribbean; e.g., Braszus et al., 2021; Harris et al., 2018; van Benthem et al., 2013; Zhu et al., 2020).

constant dip down to $\sim 1,500$ km depth. Conversely, Atlantic subduction below the LA is shallower and confined mainly to the upper mantle (Figure 1b).

Throughout the Cenozoic, internal deformation of the Caribbean plate has been relatively limited. Traces of young backarc extensional basins or other indications of major internal deformation are limited to the Granada basin in the eastern portion of the plate and large-scale ($> 2,000$ km) strike-slip fault zones. Two such fault systems form the northern and southern boundaries of the Caribbean plate (Burke, 1988; Mann & Burke, 1984). To the north, deformation is localized along the Cayman Spreading Center and the Oriente-Septentrional fault and Walton-Enriquillo-Plantain Garden fault systems, which merge laterally into the PR and Muertos trenches. To the south, deformation is accommodated by the Southern Caribbean Deformed Belt, producing subduction of the

Caribbean beneath South America, and transpressional deformation along the Oca-San Sebastian-El Pilar fault system (Figure 1a).

Figure 2 shows the reconstructed Cenozoic evolution of the Caribbean plate in the hybrid hot-spot reference frame of Müller et al. (2019). The colored polygons represent the plate margins extracted from the Müller et al. plate reconstruction model using *GPlates* (Müller et al., 2018). We slightly modified the 50 Ma–38 Ma plate topologies in the eastern Caribbean to reflect new constraints on Granada opening from Garroq et al. (2021), assuming constant spreading rates. The trajectory of the Farallon and North American plates relative to the Caribbean plate is shown in the inset in Figure 2a, highlighting the shift in relative motion of the North American plate between 50 and 30 Ma. The reconstruction is superimposed on a 900 km depth slice of the UU-P07 *P*-wave tomography model (Amaru, 2007; Hall & Spakman, 2015) to show the slab anomalies in the upper mantle that presumably resulted from Farallon/Cocos, GAC, and LA subduction (Figure 4b). In the rightmost panels, we show the configuration of the northern and eastern Caribbean plate margins in the Paleocene just prior to the reorganization (Figure 2c), in the middle Eocene during the transition (Figure 2d), and in the early Miocene after the reorganization (Figure 2e).

Geochronological constraints from magmatic rocks along the northern Caribbean margin (Figure 3) indicate that Cretaceous to Paleogene subduction related to the GAC was active until the early-middle Eocene (Figures 2a–2c and 3; e.g., Jolly et al., 1998; Lewis et al., 1991; Stanek et al., 2009). The GAC was later abandoned with an interruption of subduction-related magmatism and the formation of a regional unconformity (e.g., Dolan et al., 1991; Gordon et al., 1997). As shown in Figure 3 (gray bar), the termination of GAC magmatism occurred abruptly, at ~40 Ma, in Cuba (Rojas-Agramonte et al., 2006) and Hispaniola (Escuder-Viruete et al., 2015). In PR and the Virgin Islands (PRVI), volcanism terminated somewhat later between 35–30 Ma (Smith et al., 1998). Volcanism corresponding to the eastern GAC is thought to have ended at ~60 Ma, then resumed at the LA by, at the earliest, 40 Ma (Jolly et al., 1998).

In the northern region, the Bahamas platform (Figure 1) began to subduct below Cuba, causing a surge of compression (García-Casco et al., 2008; Iturralde-Vinent, 1994). This event progressively migrated eastward to Hispaniola, where tectonic inliers comprising high pressure GAC-related assemblages are exposed alongside deep seismicity that is active today (Dolan et al., 1998). The abandonment of the northern GAC resulted in the formation of a new transform plate boundary, marked by rifting in the Cayman Trough at ~49 Ma (Leroy et al., 2000; Pubellier et al., 2000). Along this boundary, since the middle Eocene, Hispaniola and PR have hosted transpressional deformation over inward dipping subduction of both the Atlantic and Caribbean (Muertos Trough) lithospheres (Dolan et al., 1998). Most onshore strike-slip deformation is localized in northern and southern Hispaniola (Calais et al., 2016).

At the eastern boundary of the Caribbean seafloor, ~300 km west of the LA arc, is the largely submarine Aves Ridge. Though poorly investigated, it has been interpreted as the abandoned eastern portion of the GAC, which was potentially active until ~60 Ma (Neill et al., 2011). This interpretation is supported by wide angle seismic studies showing that the ~25 km-thick crust beneath the Aves Ridge has a velocity structure compatible with an arc origin (Christeson et al., 2008; Padron et al., 2021). However, the interval between the abandonment of the GAC and the onset of LA subduction is not well documented.

The Granada Basin, east of the Aves Ridge, is thought to be a back-arc basin with a highly oblique (~30° to the trench), NW-SE trending, spreading phase of ~200 km during the early to middle Eocene (Garroq et al., 2021). Figure 2d shows a simplified schematic of the basin during this time. The presently active LA arc extends from the Venezuelan continental margin to the Agada Passage between PR and the Virgin Islands. The edifice is constructed upon an extinct Cretaceous arc that can be observed on La Désirade Island in the northern LA offshore of Guadeloupe (Bouysse & Guennoc, 1983; Corsini et al., 2011; Neill et al., 2010). Studies of the LA arc and Granada Basin suggest that an episode of renewed subduction along the eastern GAC trench lead to intra-arc extension, forming the Granada Basin, and separating the active LA arc from the remnant arc, the Aves Ridge (Bird et al., 1999; Bouysse, 1988; Pindell & Barrett, 1991). Concurrently, the LA forearc shifted several 100 s of km parallel to the trench, rotating blocks further west around the cusp of the arc (Montheil et al., 2023). At this time, the southern boundary of the Caribbean plate was mainly characterized by oblique to strike-slip deformation between the extinct southern end of the GAC and South America (Escalona & Mann, 2011; Pindell & Barrett, 1991; Wright & Wyld, 2011).

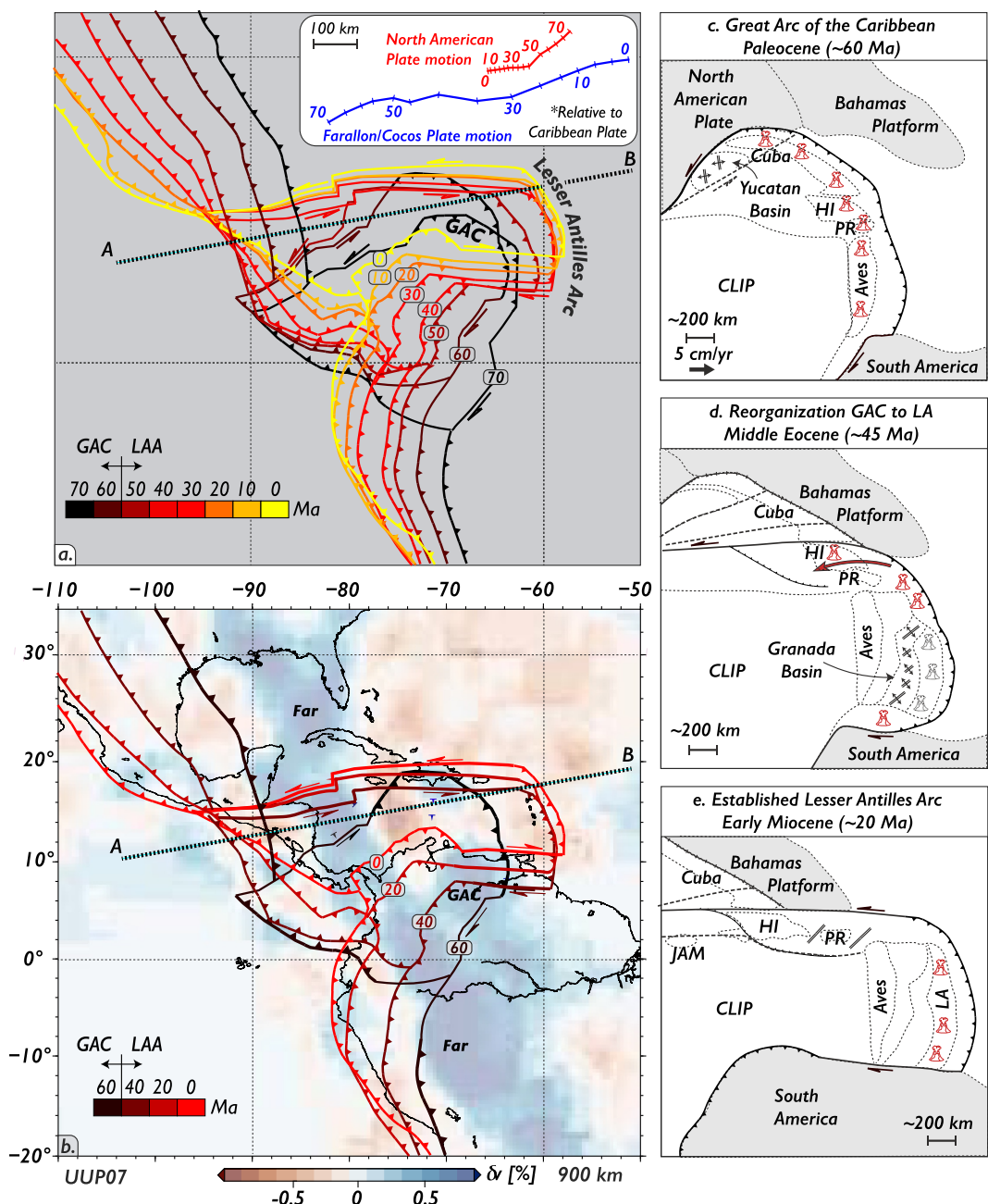


Figure 2. Simplified reconstruction of the Caribbean realm. (a) Evolutionary scenario in a mantle reference frame proposed for the Cenozoic evolution of the Caribbean margin (modified after Müller et al., 2019, accounting for Granada basin opening following Garroq et al., 2021). The inset shows the motion of the leading edge of the Farallon and North American plates relative to the Caribbean plate from 70 Ma onwards. Note the plate reorganization between 50 and 30 Ma, following the onset of west-dipping subduction at the Lesser Antilles (LA) arc and abandonment of the Great Arc of the Caribbean (GAC). The thick dashed line shows the location of the tomographic section in Figure 1. Colored lines correspond to the reconstructed time (see legend). (b) Evolutionary scenario superimposed on seismic tomography at 900 km depth (UUP07 of Amaru, 2007), showing slab anomalies in the upper lower mantle. Symbols same as in (a). (c–e) Illustrations of the GAC and LA portions of the Caribbean region in the (c) Paleocene, (d) middle Eocene, and (e) early Miocene. Symbols show basin opening (black bars with diverging arrows), recorded volcanism (red volcano icons), inferred volcanism (black volcano icons), and the supposed locations of Cuba, the Bahamas platform, the Yucatan Basin, the North and South American Plates, Hispaniola (HI), Puerto Rico, the Aves Ridge, and the Caribbean Large Igneous Province. Solid black lines show fault locations, dotted lines show boundaries between tectonic features, bold dashed lines show incipient or former fault zones, and the hatched line shows the suture zone between Cuba and the North American plate. The red arrow in (c) shows the rotation of the LA forearc sliver from Montheil et al. (2023). Drawn after Cerpa et al. (2021), Garroq et al. (2021), and Pindell and Kennan (2009).

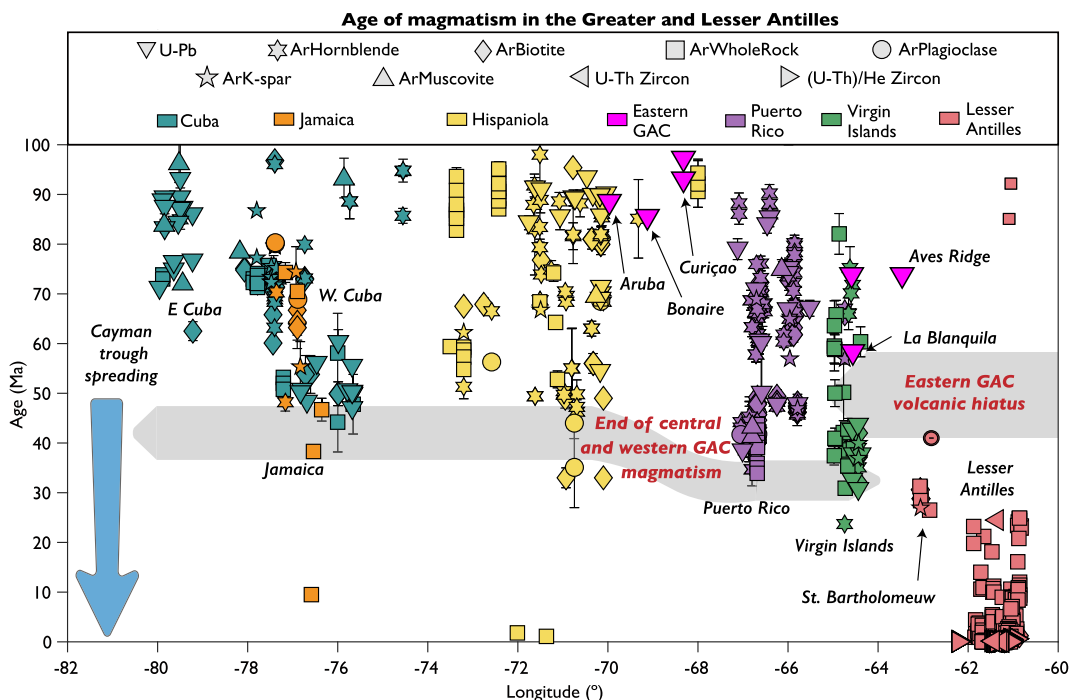


Figure 3. Zircon U-Pb, K-Ar, $^{40}\text{Ar}/^{39}\text{Ar}$, U-Th, and (U-Th)/He (minerals listed on the plot; K-Ar and $^{40}\text{Ar}/^{39}\text{Ar}$ reported together) data from the Greater and Lesser Antilles (LA), the Aves Ridge, and southern Caribbean islands showing the late Eocene cessation of Great Arc of the Caribbean (GAC) volcanism and initiation of LA volcanism. Error bars are shown for data points with errors larger than the symbol size (~ 2 Ma). Geo- and thermochronometric data from a compilation by Wilson et al. (2019) and the EarthChem Portal (<http://www.earthchem.org>). The end of the GAC magmatism (gray bar) after Rojas-Agramonte et al. (2006) for Cuba, Escuder-Viruete et al. (2015) for Hispaniola, and Smith et al. (1998) for Puerto Rico. Note that the ages reported below this point likely do not reflect GAC magmatism but instead are offset by the time between crystallization and cooling until the mineral closure temperature (e.g., $^{40}\text{Ar}/^{39}\text{Ar}$ Plagioclase age from Escuder-Viruete et al., 2015), partial radiogenic Ar loss (e.g., K-Ar Biotite age from Kesler et al., 1991), or otherwise reflect quaternary volcanism associated with extensional tectonism (Kamenov et al., 2011). The timing of initiation of Cayman trough spreading is from Leroy et al. (2000).

The post-reorganization Caribbean system (Figure 2e) resembles the present-day tectonic configuration, with the formation of the northern and southern transform faults and the onset of west-dipping subduction at the LA. After the prolonged north-to-northeastward drifting phase and eastward shift in motion, from ~ 40 Ma onward, the Caribbean plate remained nearly stationary in an absolute reference frame (Figures 2a and 2b; Boschman et al., 2014).

3. Slab Dynamics and the 4-D Evolution of the Caribbean

3.1. Tectonic Constraints on the Evolution of Caribbean Subduction

Several models attempt to explain the Paleogene Caribbean reorganization, though they frequently disagree on the precise timing. Most authors propose a gradual transition from the GAC to LA during the Eocene (e.g., Boschman et al., 2014; Escalona et al., 2021; Lidiak & Anderson, 2015; Pindell & Kennan, 2009, and references therein), citing the onset of spreading in the Cayman trough as the main constraint (Leroy et al., 2000). To be consistent with geological and geophysical constraints, any proposed model must consider the following:

1. After a prolonged quasi-stationary period, the Pacific trench and the Caribbean plate advanced eastward during the Eocene for ~ 500 km.
2. The primary magmatic phase in the central and western GAC began waning from ~ 55 Ma with termination by ~ 40 Ma (Cuba, Jamaica, Hispaniola), followed by intermediate magmatism in PR and the Virgin Islands until ~ 35 Ma. In the eastern GAC (Aves Ridge, and southern Caribbean islands) volcanism ceased at ~ 60 Ma then resumed between 35 and 40 Ma (LA, Figure 3).

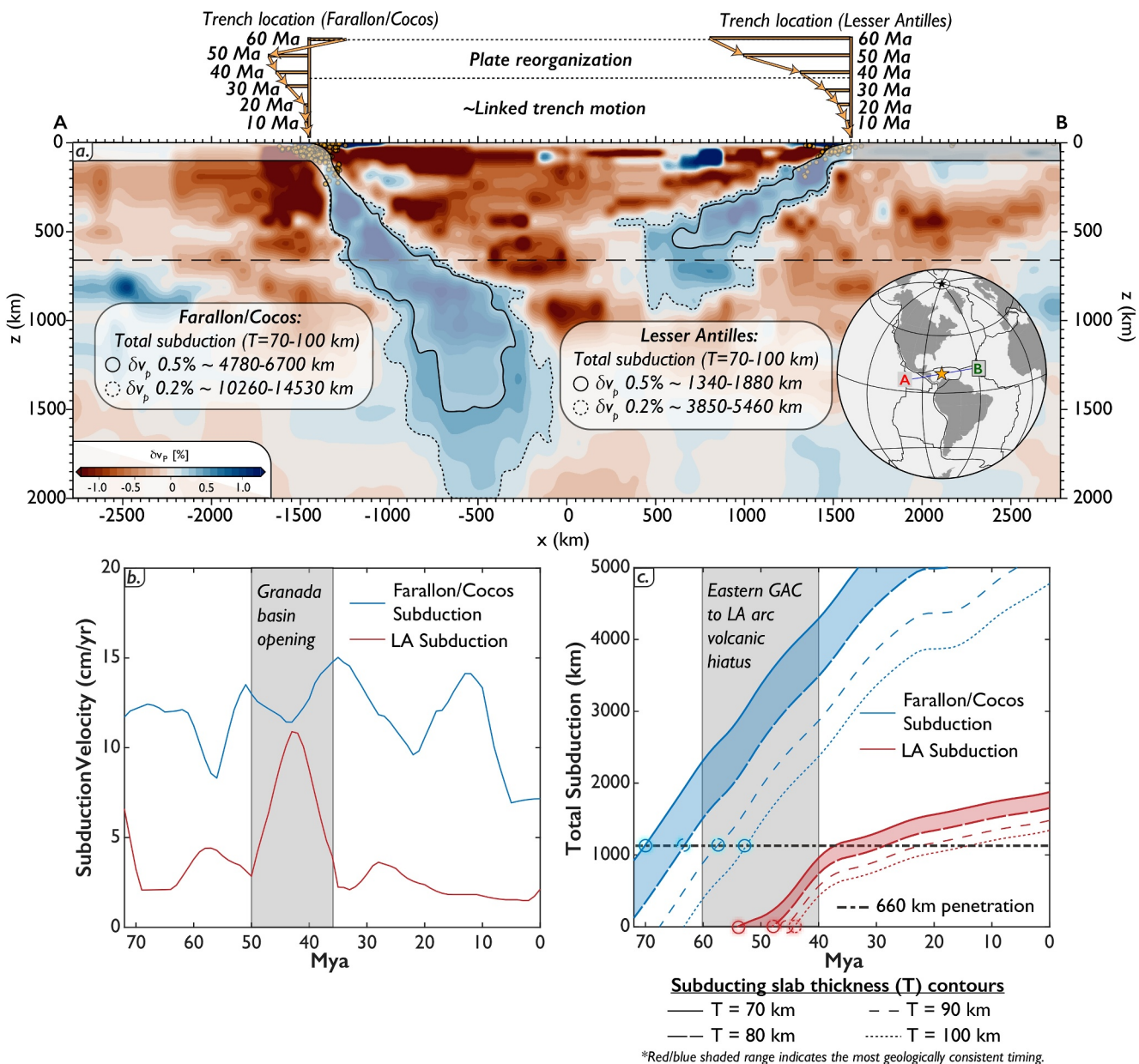


Figure 4. Tomographic analysis and reconstruction of subducted material at the Farallon/Cocos and Lesser Antilles (LA) subduction zones. (a) Tomographic cross-section (line shown in Figure 1) with measured δv_p anomalies and corresponding amounts of subduction assuming a plate thickness of 70–100 km and $\delta v_p = 0.5\%$. The tree structures on the top of the figure represent trench motion measured from the reconstruction in Figure 2. (b) Subduction velocities through time for the Farallon/Cocos (blue) and LA (red) from the Müller et al. (2019) plate model modified to incorporate Granada basin spreading estimates from Garroq et al. (2021) (gray box). (c) Reconstructed total amount of subduction through time for the Farallon/Cocos (blue) and LA (red). Contours represent different selections of subducting slab thicknesses (T). The gray box shows the approximate timing of the eastern Great Arc of the Caribbean volcanic hiatus (Jolly et al., 1998). Colored circles show the timing of Farallon lower mantle penetration and the onset of LA subduction. Semi-opaque red and blue areas reflect the most geologically consistent timing.

3. The Granada Basin opened highly obliquely, approaching a nearly trench parallel direction (~200 km net extension; Garroq et al., 2021) in the middle Eocene, and the PR-Virgin Islands forearc sliver migrated along the LA trench, suggesting that the trench was locked or stationary at that time (Montheil et al., 2023).
4. Seafloor spreading in the Cayman trough began at ~49 Ma (Leroy et al., 2000), indicating that a plate boundary resembling the present-day northern Caribbean was already established (Leroy et al., 2000).
5. There was a Greater Antilles-wide late Eocene-Oligocene unconformity marking the tectonic reconfiguration of the western and central GAC (e.g., Dolan et al., 1991; Gordon et al., 1997).

The considerations listed above indicate that the entire plate margin was reshaped, establishing new plate boundaries, with a rapid eastward drift of an almost undeformed Caribbean plate from the late Paleocene to early Oligocene (Boschman et al., 2014). During the transition, the eastern GAC was abandoned with volcanism ceasing at \sim 60 Ma. From 40–25 Ma, the emerging LA arc was potentially reactivating the magmatic potential of the eastern extent of the residual GAC slab. Lastly, from 25 Ma onward, LA arc magmatism was fully established along its length (Figure 3). However, the principal drivers of plate reorganization and the onset of LA subduction remain unclear.

3.2. The Bahamas Platform Collision and Escape Model

Most previous models suggest that the entrance of the Bahamas platform into the GAC trench was the leading cause of the Paleogene plate reorganization. In this scenario, subduction at the LA is a result of the eastward escape of the Caribbean plate (e.g., Boschman et al., 2014; Mann et al., 1995; Pindell & Kennan, 2009). Evidence for the Bahamas platform collision model includes the present-day location of Cuba on the North American plate, comparatively large thrust earthquakes and anomalous bathymetry in the deformed belt north of Hispaniola (Dolan et al., 1998), the Greater Antilles wide late Eocene unconformity (e.g., Dolan et al., 1991; Gordon et al., 1997), and the spreading record in the Yucatan basin (Rosencrantz, 1990) and the Cayman trough (Leroy et al., 2000). However, this evidence is also compatible with our slab interaction model outlined below, which does not prohibit a partial role for the Bahamas platform in shaping the northern Caribbean.

The Bahamas platform collision and eastward escape model on its own faces some inconsistencies related to how deformation progressed across the GAC during the Eocene (Cerpa et al., 2021). These include:

1. In Hispaniola, contractional deformation began in the mid-late Eocene (Dolan et al., 1991; Heubeck et al., 1991; Huerta & Pérez-Estaún, 2002; Pubellier et al., 2000) synchronously with compression in PR (La-Dávila, 2014; Román et al., 2020) and back thrusting along the Muertos fold-and-thrust belt (Granja Brúna et al., 2014). The opening of the Cayman trough (Leroy et al., 2000) and Granada basin (Aitken et al., 2011; Garrocq et al., 2021) preceded these shortening episodes and the Oriente-Septentrional fault was already active (de Zoeten & Mann, 1991), suggesting that northern Caribbean deformation occurred after the new plate configuration was established.
2. Aside from a late Eocene backthrusting episode in Hispaniola (Mann et al., 1991), there is no clear trace of a large-scale pre-Neogene compressional episode in the central Greater Antilles nor a record of accreted Bahamas platform material (Mann et al., 1991), suggesting that compression may only be caused by a “soft-collision” with the Bahamas platform, if at all influenced by this event (Cerpa et al., 2021; van Benthem et al., 2014). Turbidite deposition in northern Hispaniola further attests to relatively uninterrupted deposition in a deep trench that existed from the late Eocene to the middle Miocene (de Zoeten & Mann, 1991; Dolan et al., 1991).
3. Blueschist facies metamorphism in Hispaniola has been recorded in the late Eocene to early Oligocene (Catlos & Sorensen, 2003; Escuder Viruete & Pérez Estaún, 2004; Joyce, 1991), much later than the proposed timing of Bahamas platform collision, suggesting that subduction never fully ceased in this portion of the GAC. This is supported by the observation that convergence between the Caribbean plate and North America along the former subduction margin north of Hispaniola is still ongoing (Benford et al., 2012; Calais et al., 2016; Symithe et al., 2015).

Alternative models for central-western Greater Antilles deformation include a proposed change in the stress field induced by the corner of an arcuate trench (Cerpa et al., 2021), a “slab edge push” from the western edge of the LA slab (van Benthem et al., 2014), and “bookshelf” style compression caused by the westward motion of the Hispaniola-PRVI block (Montheil et al., 2023). These models are compatible and require the prior establishment of the LA subduction zone to provide the arcuate corner/slab edge push and drive the PRVI block rotation.

Since the record of a well-defined Bahamas platform “collision” with the central and eastern Greater Antilles before the establishment of the northern Caribbean plate boundary is absent, it is unlikely that it would have caused the eastward shift in the absolute motion of the Caribbean plate as previously thought (e.g., Boschman et al., 2014; Burke, 1988; Escalona et al., 2021). It seems that many of the late Eocene-present tectonic events in the Greater Antilles and LA are instead influenced by the presence of the pre-existing, highly arcuate LA subduction front (Cerpa et al., 2021).

3.3. Total Subduction Length Estimates From Seismic Tomography

Mantle tomography may provide useful information to unravel the tectonic history of the margin (e.g., Chen et al., 2024; Hafkenscheid et al., 2006; van Benthem et al., 2013). Here, we explore the relationships between the Farallon and LA slabs by using tomography to estimate the slab length beneath each subduction zone. These estimates can then be compared with the expected amount of subduction from plate models to reconstruct the history of subduction through time. To do this, we use the UU-P07 P -wave tomographic model (Amaru, 2007; Hall & Spakman, 2015) and analyze structure within a cross-section that is near-perpendicular to the LA and Farallon trenches and is also near-parallel to the trajectory of the subducted North American and Farallon plate lithosphere (Figure 2). Following these specifications, and using the slab architectures proposed in previous studies (e.g., Braszus et al., 2021; van Benthem et al., 2013; Zhu et al., 2020), we select a profile (center point: 75°W, 15°N, azimuth: 80° CW from N) that best captures the full extent of subduction at both trenches, with continuous and well-resolved anomalies, allowing their relationship to be analyzed in a 2-D approximation (Figure 4a).

We evaluate the amount of total subduction using the area of the tomographic section with relative P -wave velocity anomalies, δv_p , less than a specified anomaly value. By dividing this area by a range of oceanic lithosphere thicknesses (70–100 km), we arrive at approximations of total slab length. Our results indicate that for plate thicknesses between 70 and 100 km, there are 4,780–6,700 and 10,260–14,530 km beneath Central America (CAM) and 1,340–1,880, and 3,850–5,460 km beneath the LA for the 0.5% and 0.2% δv_p , contours, respectively.

To reconstruct the amount of subduction through time, we use the Müller et al. (2019) plate model corrected by trench motion using new constraints from Garroq et al. (2021). We use the kinematics tool in *GPlates* to track the convergence between the Caribbean plate (*GPlates* plate-ID: 2007) and North American (ID: 101) and Farallon/Cocos (ID: 902/909) plates (Müller et al., 2019). For Farallon/Cocos subduction, we use the relative motion between the Caribbean and the leading edge of the Farallon/Cocos in the Müller et al. (2019) model. To account for trench motion in the LA, we manually extract the relative velocity between the North American and Caribbean static plates and adjust this using trench motion estimates deduced from the mid-Eocene extension record in the Granada basin along a similarly oriented cross-section (Garroq et al., 2021).

Our calculations suggest that for the total subduction length estimates corresponding to the 0.5% δv_p contours listed above, the Farallon slab penetrated the lower mantle at 52–70 Ma, followed by the later onset of subduction at the LA by 44–54 Ma. This analysis relies on two key assumptions: (a) that the mostly palinspastic and geologically constrained reconstruction of Müller et al. (2019) is valid within the scope of our study, and (b) that subducted material related to the LA and the most recent phase of Farallon/Cocos subduction are interpretable as continuous velocity anomalies in the lower mantle above the determined δv_p threshold. We attribute additional, disconnected material typically residing in the lower mantle to the phase of subduction prior to ~100 Ma (Riel et al., 2023) for the Farallon and to eastern GAC subduction for the LA (Neill et al., 2011). Following the tomographic interpretations in Zhu et al. (2020) and Braszus et al. (2021), the selected profile does not cross this material. We discuss and refine our estimates in the context of both geological constraints and tomographic assumptions below.

3.4. Geodynamic Models

3.4.1. Model Setup

To explore whether slab penetration into the lower mantle is a dynamically feasible mechanism for plate reorganization, including subduction initiation in the overriding plate, we constructed time-evolving, 2-D thermo-mechanical numerical subduction models. To solve the equations governing conservation of mass, momentum, and energy, we use the *ASPECT* finite element code (version 2.4.0; Bangerth et al., 2023; Heister et al., 2017; Kronbichler et al., 2012). The approach generally follows our earlier work (cf. Faccenna et al., 2021; Holt & Condit, 2021). We provide an overview of the model setup below; details can be found in Supporting Information S1.

We consider a whole mantle domain with free slip boundaries and initiate the system by prescribing an initial thermal proto-slab extending to 250 km depth (Figure 5a). Our subduction system consists of three lithospheric plates. The left-most subducting plate, including the initial proto-slab, is purely a thermal lithosphere with an initial age of 60 Ma (as defined by a halfspace cooling profile). The middle plate, which overrides the left-most

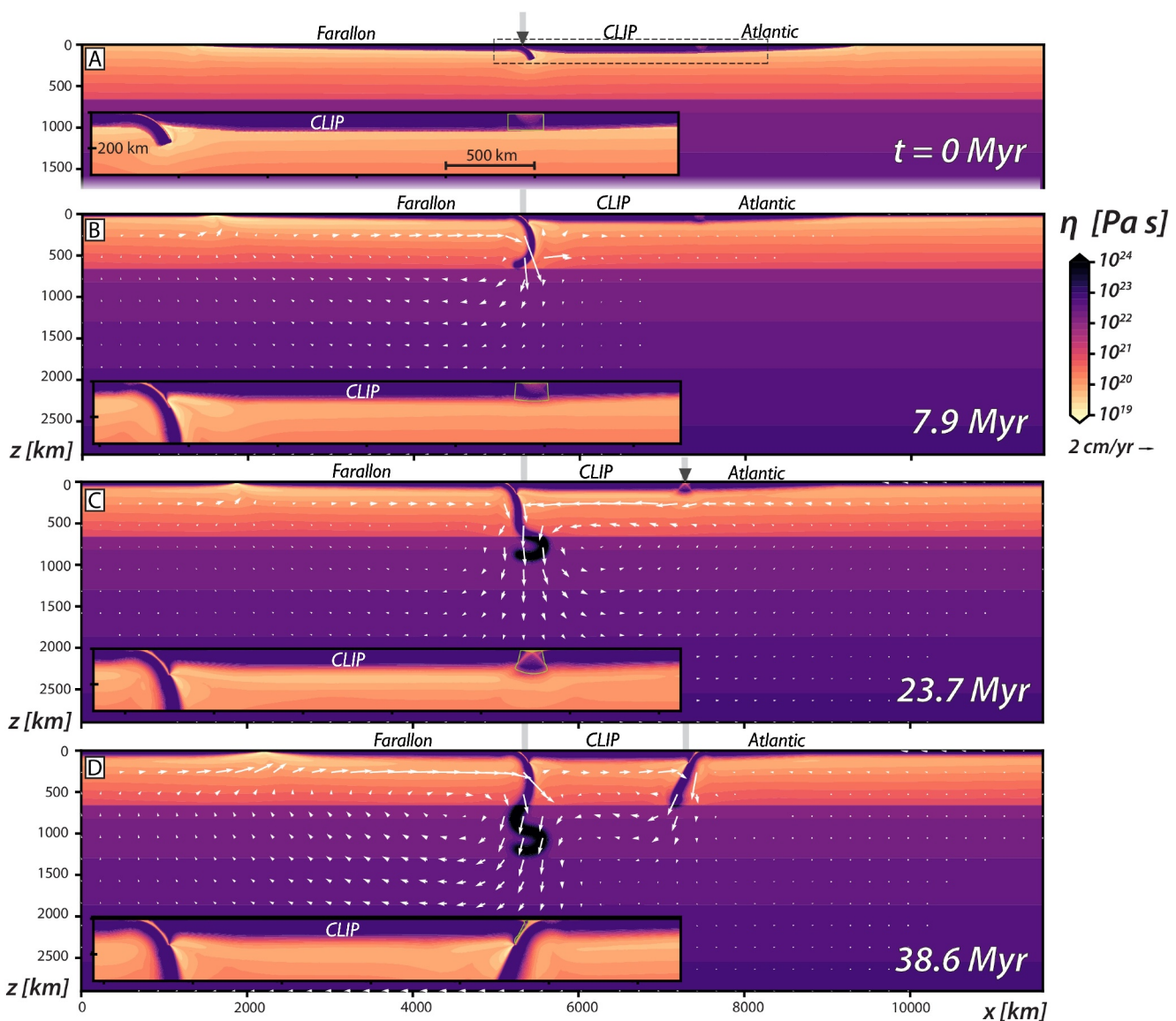


Figure 5. Numerical subduction model illustrating the initiation of a subduction zone along a weak margin (originally at 7,000 km from the trench) due to penetration of an oppositely dipping slab in the lower mantle. (a) Initial viscosity structure. (b–d) Slab evolution at three illustrative phases—(b) lower mantle impingement, (c) subduction initiation, (d) and mature subduction of the oppositely dipping slab—with the viscosity field and mantle flow vectors plotted for each time. Zoomed-in insets show the subduction initiation process in more detail, with the weak zone (low yield stress) material outlined in light green. Labels above the plots and within insets indicate how the model setup corresponds to the Caribbean subduction scenario.

subducting plate and is 2,000 km long, mimics the Caribbean LIP (CLIP) in that it has a greater thickness (thermal age of 100 Ma) and a reduced lithosphere density ($\Delta\rho = 75 \text{ kg/m}^3$) relative to the “regular” oceanic lithosphere on either side of it. To the right, the CLIP transitions again to purely thermal oceanic lithosphere, which is of 100 Ma age and represents the Atlantic. Our models evolve dynamically so that no external forces/velocities are applied.

We used a composite diffusion creep, dislocation creep, and pseudo-plastic rheology. Plastic yielding operates within the lithospheric plates, dislocation creep in the upper mantle to average depths of ~ 250 km, and the lower mantle is exclusively diffusion creep (see Figure 5 for the effective viscosity, η , distribution that results). Parameters used for dislocation and diffusion creep flow laws are consistent with the range of experimental values determined for dry olivine (Hirth & Kohlstedt, 2003; Karato & Wu, 1993). The upper to lower mantle transition, at 660 km depth, is imposed as a viscosity jump of 25 (cf. Hager, 1984).

Yielding reduces the model viscosity in regions of high deviatoric stress to a depth-dependent yield stress (e.g., Enns et al., 2005; Moresi & Solomatov, 1998). Our imposed yield stress, σ_y , increases with pressure (\approx depth) via a coefficient of quasi friction ($\sigma_y = \mu P$), and is capped at 0.5 GPa. In the oceanic lithosphere, μ is set to 0.3 (cf. Bellas & Zhong, 2021; Garcia et al., 2019; Sandiford & Craig, 2023). The left-most subducting plate and protol slab are decoupled from the middle plate by a crustal layer that is thin (7.5 km), weak (viscosity 10^{20} Pa s), and positively buoyant ($\Delta\rho = 200$ kg/m³ relative to background material). The crust rests on top of all plates and, in subduction zones, is eliminated at depths beyond 100 km (e.g., Holt & Condit, 2021).

Relative to Faccenna et al. (2021), we add a vertical weak zone at the boundary between the middle and rightmost plates (i.e., the CLIP-Atlantic boundary). This zone is 200 km wide, cuts through the 100 km-thick lithosphere, and has a reduced plastic yield strength of $\mu = 0.013$ (\sim 5% of the ambient strength) in our reference model. This corresponds to a mid-lithospheric (40 km depth) σ_y of 17 MPa. This strength anomaly is intended to represent the eastern edge of the GAC subduction margin, thought to be the trench, presumably to the east of the Aves Ridge. The Aves Ridge may be underlain by oceanic crust similar to the Venezuelan Basin (Neill et al., 2011), which formed prior to the CLIP (Mauffret & Leroy, 1997). About two-thirds of recently formed subduction zones appear to initiate at the transition between oceanic and arc or plateau lithosphere (Lallemand & Arcay, 2021). The change from Aves Ridge arc lithosphere to oceanic lithosphere, associated with a former subduction plate boundary, may represent a prior weak zone which can then be reactivated for subsequent subduction initiation (cf. Fuchs & Becker, 2019). We examine the impact of various levels of yield strength reduction in this zone for a range of inherited weak zone strengths ($\sigma_y(40$ km) = 11–46 MPa) in Supporting Information S1.

3.4.2. Model Dynamics

In our reference model (Figure 5), the slab tip hits the upper to lower mantle viscosity jump after \sim 8 Myrs and then proceeds to fold and penetrate through the viscosity discontinuity between 8 and 15 Myrs into the model run. As the slab penetrates into the lower mantle, subduction-induced mantle return flow transitions from being mainly confined to the upper mantle to spanning the entire mantle, thereby increasing the magnitude of basal tractions that drag the upper plate into the subduction trench (Figure 5b; cf. Faccenna et al., 2021; Yamato et al., 2009).

After 24 Myrs of model evolution, and \sim 15 Myrs after slab impingement on the lower mantle, large-scale flow is sufficiently vigorous to induce basal tractions beneath the upper plate that in turn drags the upper plate toward the relatively stationary, or “anchored,” Farallon slab. This causes the upper plate stress state to become more compressional and subsequently initiates oppositely dipping subduction (Figure 5c). The 75 kg/m³ increase in density along the passive margin, from the CLIP to the Atlantic plate, induces a lithostatic pressure gradient that pushes on the Atlantic, thereby also providing an important additional source of horizontal compression (e.g., Faccenna et al., 1999; Nikolaeva et al., 2010). Hence, subduction initiation occurs once the stress associated with both mechanisms overcomes the weak zone yield strength (Figure S1 in Supporting Information S1). The new subduction zone initiates after the original (left-most) slab has penetrated to \sim 1,000 km depth and itself reaches the base of the upper mantle (i.e., close to the present day slab geometry; Figure 4a) after \sim 40 Myrs of model evolution (Figure 5d).

In addition to initiating subduction with a polarity that is consistent with the regional tectonics, the directions of our modeled trench motions agree, to first order, with the Caribbean reconstruction: Before the initiation of the rightmost (LA) slab, the left-most (Farallon/Cocos) trench retreats (Figure 5). After LA initiation, the Farallon/Cocos trench switches its trench motion direction from retreat to advance, and the LA trench retreats. This switch in Farallon/Cocos trench motion occurs after the Caribbean slab has reached \sim 200 km depth and thus has sufficient net negative buoyancy to drag the entire subduction system right-wards.

The link between deep mantle subduction, whole mantle scale flow, and upper plate compression has been explored previously in time-dependent subduction modeling studies (e.g., Faccenna et al., 2017, 2021; Yang et al., 2018). Our study also follows from previous work demonstrating the active role of large-scale mantle flow in initiating and sustaining subduction zones (e.g., Baes et al., 2018; Pusok & Stegman, 2019; Yamato et al., 2013). This includes the proposition that slab penetration-induced mantle flow may have also initiated the Scotia subduction zone farther south (Schellart et al., 2023).

To explore the conditions required to initiate oppositely dipping subduction, we conducted additional tests varying the weak zone yield strength ($\mu = 0.009$ to 0.35) and CLIP density anomaly ($\Delta\rho = 25$ –100 kg/m³) relative

to our reference model. Holding the CLIP density contrast fixed to 75 kg/m^3 and reducing the weak zone yield strength ($\mu = 0.009$; $\sigma_y(40 \text{ km}) = 11.5 \text{ MPa}$) results in delamination of the weak zone material and hence no initiation of the second subduction zone (Figure S2a in Supporting Information S1). A moderate increase in weak zone strength ($\mu = 0.017$; 23 MPa) results in very sluggish subduction initiation, with partial subduction of the upper plate, which ultimately stalls (Figure S2c in Supporting Information S1). A greater increase ($\mu = 0.035$; 46 MPa) renders the weak zone too strong to yield (Figure S2d in Supporting Information S1). Increasing the CLIP density anomaly to 100 kg/m^3 or decreasing it to 50 kg/m^3 does not change the overall evolution but causes LA subduction to initiate faster or slower, respectively (Figures S3b, S3d, S4b, and S4c in Supporting Information S1). Further decreasing $\Delta\rho$ to 25 kg/m^3 causes very sluggish subduction initiation (Figure S3a in Supporting Information S1), and subduction does not initiate in models without a density contrast between the CLIP and the Atlantic.

These tests demonstrate the importance of the along-strike density gradient at the CLIP-Atlantic boundary (cf. Li & Gurnis, 2023; Mueller & Phillips, 1991; Nikolaeva et al., 2010; Toth & Gurnis, 1998). If the CLIP has a density comparable to the Atlantic, subduction will not initiate, despite the increase in compression as the Farallon slab penetrates the lower mantle and greater compressive stress in the interior of the CLIP (Figure S4 in Supporting Information S1). In contrast, a larger density contrast drives greater compression within the weak zone (i.e., at the CLIP-Atlantic density jump), which when combined with a slab penetration-induced increase in basal traction, initiates subduction (Figure S4 in Supporting Information S1). The onset of subduction due, in part, to density contrasts is also broadly analogous to the suggestion of Riel et al. (2023) that a prior phase of Cretaceous Farallon subduction was initiated due to the juxtaposition of the early Cretaceous part of the buoyant CLIP with oceanic lithosphere. Riel et al. proposed that later interactions between the east-dipping Farallon slab and west-dipping proto-Caribbean slab lead to trench retreat, back-arc spreading, and the generation of an upper-mantle plume that corresponds to a second, Late Cretaceous, generation of CLIP activity.

Our models thus demonstrate the feasibility of slab anchoring-induced subduction within a Caribbean plate tectonic geometry. Such an evolution occurs only over a relatively narrow range of effective weak zone strengths but a broad range of CLIP densities. More sophisticated models (e.g., with more complete lithospheric rheologies), and a broader parameter space exploration, are needed to further characterize the robustness of this regional subduction initiation mechanism. Those tests should ideally include 3-D mantle convection models that can account for effects such as lithospheric thickness variations, which may significantly affect mantle flow in the southern part of our study region (e.g., Miller & Becker, 2012).

4. Discussion

4.1. Dynamically Driven Tectonic Evolution of the Caribbean

Our numerical models (Figure 5) and results from previous work (e.g., Faccenna et al., 2017; Husson et al., 2012; Yamato et al., 2013; Yang et al., 2016) suggest that the penetration of a subducting slab into the lower mantle causes in-plane compression in the upper plate. The presence of both a pre-existing weak zone and a lithospheric density contrast in the upper plate facilitates the localization of contractional deformation leading to the initiation of an inward dipping subduction system (Figure 5). From these results, we propose that the penetration of the Farallon/Cocos slab in the latest Cretaceous to Paleocene caused a surge of compression across the Caribbean plate, which by the middle Eocene reactivated the dormant abandoned GAC trench (Aves Ridge), and resulted in the subduction of the Atlantic lithosphere at the LA.

According to the proposed model, slab anchoring should result in upper plate compression, initially along the CAM trench and then propagating laterally eastward. Several cycles of uplift and subsidence have been documented in basins on and offshore CAM (Brandes & Winsemann, 2018). Brandes and Winsemann largely attribute compression and uplift documented in forearc basins to the changes in subduction conditions, mainly the subduction of aseismic ridges, yet slab anchoring would have similar consequences. In a slab anchoring as a driver interpretation, early Paleocene uplift described in Costa Rica (Winsemann, 1992), or the major Paleocene erosional surfaces described in several regions in Panama (Kolarsky et al., 1995; Winsemann, 1992), around the Nicaragua rise (Escalona et al., 2021), and farther south in the San Jacinto fold and thrust belt (Mora et al., 2017) and the Eastern Cordillera in Colombia (Siravo et al., 2018) could be interpreted as related to a compressional surge induced by slab dynamics.

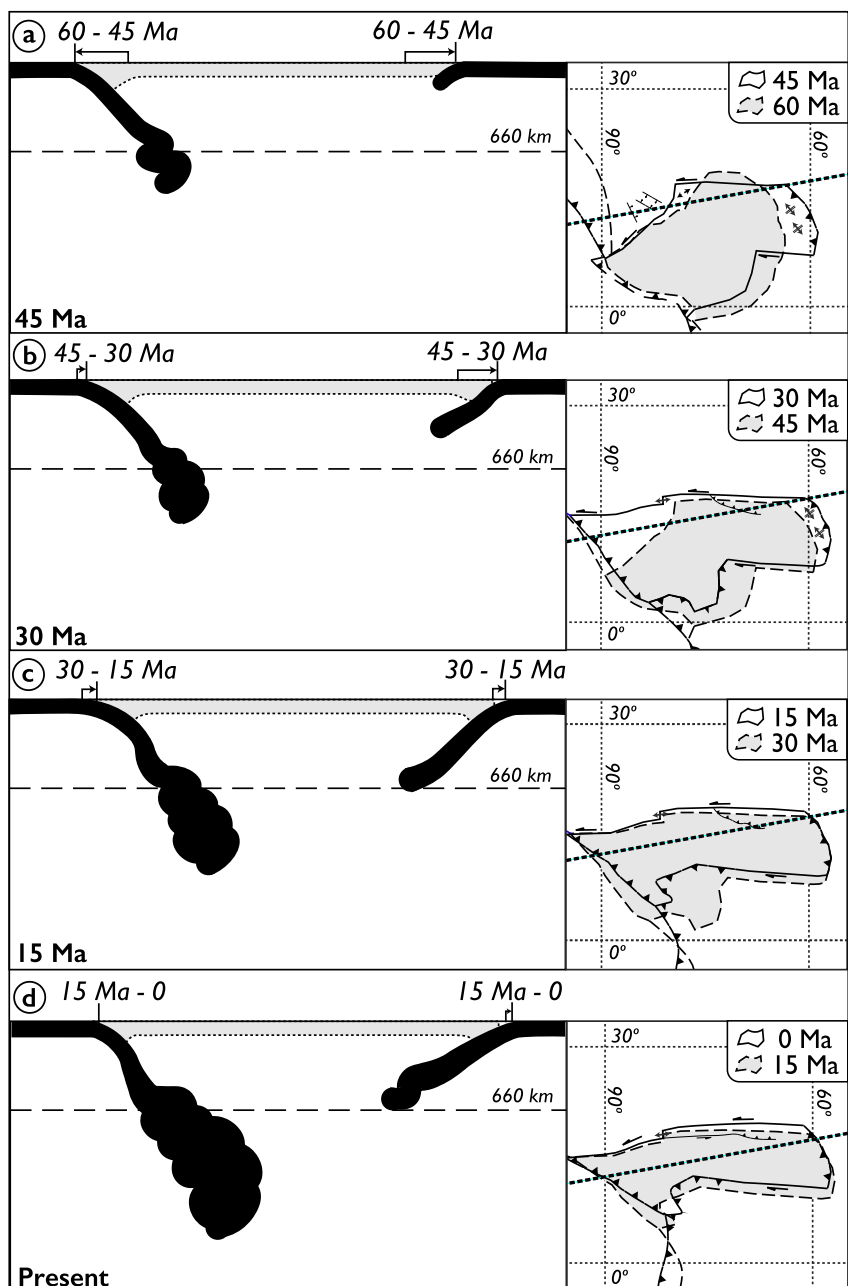


Figure 6. Schematic illustration showing the evolution of the Farallon/Cocos and Lesser Antilles (LA) subducted slab and corresponding map view reconstruction. (a–d) 15 Myr snapshots since 45 Ma. These panels show the scenarios following Farallon slab penetration into the lower mantle, corresponding to the rapid trench jump and beginning of subduction at the LA arc. Arrows above the left plots show the approximate change in trench location over the previous 15 Myrs. Note that material related to subduction at the Great Arc of the Caribbean is omitted for simplicity. On the right plots, the light gray polygon represents the plate configuration 15 Myrs prior. The gray polygon outlined by a dashed line is the configuration for the time period prior to that represented on the cross-section-view panels. The map-view reconstruction was modified after Müller et al. (2019).

Our proposed reconstruction (Figure 6) indicates that subduction re-initiated in roughly the same location as the eastern extent of the GAC trench between \sim 45–55 Ma and during the \sim 20 Myrs long magmatic pause in the eastern GAC from \sim 60 Ma to \sim 40 Ma (Figure 3; e.g., Lallemand & Arcay, 2021). The eastward younging of magmatic ages in the central and western GAC (Figure 3) may therefore reflect the decay of volcanism corresponding to the reshaping of the GAC boundary around its eastern corner to west-dipping subduction at the LA

trench. During the early phase of subduction initiation, the LA slab slightly retreated leading to middle Eocene extension in the Granada Basin (Aitken et al., 2011; Garrocq et al., 2021). In this scenario, the LA represents a case of episodic subduction (cf. Crameri et al., 2020) with a new phase initiating at the same location and with the same polarity as a preexisting subduction zone.

Based on the few samples recovered from the Aves Ridge (Neill et al., 2011) and its subaerial exposure on La Blanquilla island (Figure 3; Wright & Wyld, 2011), some authors indicate that subduction never ceased during the transition from the GAC to LA (e.g., Garrocq et al., 2021; Lallemand & Arcay, 2021). They suggest that subduction related rocks from 60 to 40 Ma were buried beneath the Granada Basin or beneath the LA forearc during a period where the position of the LA arc was further east than the present day (Allen et al., 2019).

In our model, we suggest a discontinuous subduction history, matching the presence of the well documented GAC-wide unconformity (e.g., Dolan et al., 1991; Gordon et al., 1997) and apparent interruption of volcanism. However, we recognize that rocks of middle Eocene age may be missing due to sampling bias. In this case, while a continuous magmatic history in the eastern Caribbean does not negate our reorganization mechanism and general timing of subduction at the LA trench, we should revise our model so that the new subduction episode begins in the presence of a preexisting slab in the upper mantle. However, this would require significantly more slab material in the lower mantle related to the GAC than is apparent in tomography, requiring that a portion of the GAC be sheared off as proposed by Braszus et al. (2021).

The precise timing of subduction initiation is difficult to determine and the process may occur across a time span of several millions of years (Li & Gurnis, 2023; Nikolaeva et al., 2010; Toth & Gurnis, 1998). However, the timing of LA arc initiation should be correlated with a major episode of deformation and arc magmatism occurring in the region. In the eastern Caribbean, constraints on this period include the opening of the Granada Basin (Aitken et al., 2011; Garrocq et al., 2021), rotation of the forearc sliver (Montheil et al., 2023), Aves Ridge and LA arc volcanism (Figure 3), and a regional depositional hiatus (Cornée et al., 2020; Legendre et al., 2018).

Unfortunately, the timing of these events is not well defined. For example, the age of arc volcanism at the Aves Ridge is still poorly constrained due to the lack of densely spaced marine sampling and possible alteration-related effects on previously reported dates (Fox et al., 1971; Neill et al., 2011). The recent re-evaluation of a dredged sample by Neill et al. (2011) yields a zircon U-Pb crystallization age of 76 ± 1.4 Ma. The regional unconformity is probably late Eocene in age but may span much of the Oligocene (Cornée et al., 2020; Legendre et al., 2018) and the onset of Granada basin rifting is inferred as older than middle Eocene (Garrocq et al., 2021). We suggest that Granada Basin spreading occurred during the nascent stages of LA initiation, following the release of compression during the counterclockwise rotation of the forearc domain (Montheil et al., 2023). The opening of the Granada basin in a nearly trench-perpendicular orientation suggests that the trench was indeed blocked and subduction was probably not well developed. However, additional age constraints are needed to refine the exact timing of the onset of rifting in the Granada Basin.

Prior to the onset of subduction at the LA, lateral compression due to slab anchoring is largely localized along the eastern margin of the upper plate around the weak zone (Figure S1 in Supporting Information S1). Applied to the Caribbean, this weak zone is representative of the Aves Ridge, the former easternmost extent of the GAC (Neill et al., 2011). This change in upper plate stresses has important implications for the 4-D evolution of the eastern Caribbean, including the potential uplift and later subsidence of the Aves Ridge, and potentially, even the biogeographical evolution of the region.

Around the time of Caribbean reorganization, paleontological findings from the LA, Greater Antilles, and Bahamas suggest that the emergence of the Aves Ridge in the Eocene facilitated the colonization of the Caribbean islands by South American terrestrial mammals (e.g., Iturralde-Vinent & MacPhee, 1999, 2023; Philippon et al., 2020). Philippon et al. (2020) discuss how the reconfiguration of the Caribbean margins could have provided an uplift mechanism that can be linked to the GAC-wide Eocene unconformity. From field evidence of middle to late Eocene shortening in the Virgin Islands, it is proposed that this subaerial exposure helped enable faunal dispersion. Cerpa et al. (2021) showed how compression at the arcuate corner of the LA could provide a mechanism for the uplift and later subsidence of land bridging the Aves Ridge and Greater Antilles. Subduction initiation is associated with a period of uplift followed by subsidence (Faccenna et al., 1999; Gurnis, 1992; Toth & Gurnis, 1998). Therefore, the dynamic slab interaction model proposed here aids in explaining the subaerial

exposure of the Aves Ridge, providing a mechanism for localized Eocene compression associated with subduction initiation, uplift along the eastern margin of the GAC, and establishment of the regional unconformity.

Caribbean tectonics during the late Eocene exhibited highly favorable conditions for subduction initiation/reactivation (cf. Lallemand & Arcay, 2021) with both a preexisting weak zone (Aves Ridge) and a mechanism for lateral compression in the upper plate. In the context of our numerical simulations, subduction beneath the Aves Ridge would have provided such a local strength reduction where another subduction episode could initiate after the anchoring of the Farallon/Cocos slab (Neill et al., 2011, and references therein). Furthermore, our estimates of total subduction at the LA and CAM subduction zones and the corresponding timing of lower mantle penetration and subduction onset, respectively, suggest that there was a link between the dynamics of Farallon/Cocos and LA subduction. We suggest that the Bahamas platform “collision” guided the localization of a new subduction-transform edge propagator fault (the NCPB more or less in its present form), but the folding and anchoring of the Farallon slab after reaching the lower mantle provided the ultimate push to initiate subduction along a new west-dipping subduction zone, the LA.

4.2. Subduction Considerations From Mantle Tomography

Using the 0.5% δv_p anomaly, the Farallon/Cocos subduction histories that are most consistent with geological constraints assume a plate thickness between 70 and 80 km, equating to a total subduction length of 5,900–6,700 km (blue shaded area in Figure 4c). At this total length, Farallon subduction initiation is projected at 73–82 Ma with anchoring at 63–70 Ma. With the same assumptions, our estimation of total LA subduction, 1,600–1,880 km, indicates that subduction began at 54–48 Ma (red shaded area in Figure 4c) ~10–20 Myrs after Farallon lower mantle penetration. This time period between slab penetration and subduction onset conforms with the ~15 Myr delay shown in numerical modeling results and indicated by tectonic constraints.

Previous studies estimate total subduction at the LA to be >1,100 km, matching the total amount of spreading at the Cayman Spreading center (Boschman et al., 2014; Chen et al., 2024; van Benthem et al., 2013). Our slab reconstruction approach is similar to the “slab unfolding” analysis of Chen et al. (2024). However, rather than reconstructing subduction using the subduction velocity, these authors “exhumed” the subducted LA slab with its eastern end fixed to the North American plate at the location of the LA trench. With this method, Chen et al. (2024) highlight the relationship between subducted fracture zones and tomographic anomalies (e.g., subduction of the Atlantic fracture zone), show that the LA slab is kinematically linked to North American plate motion, transporting the slab ~900 km since the onset of subduction at the LA, and measure a total subduction length of as much as 1,200 km. However, Chen et al. do not include intraplate deformation across the Caribbean, such as in the Nicaraguan basin (100 km E-W extension; Phipps Morgan et al., 2008) and the Grenada Basin (200 km NW-SE extension; Garroq et al., 2021) and therefore, these are minimum estimates (van Benthem et al., 2013). Solely considering extension in the Granada and Nicaraguan basins, and adding these values to the minimum total subduction constraint from the Cayman spreading center (~1,100 km), produces a number (~1,300 km) closer to our estimated range. Furthermore, reconstructing the LA slab using an estimate of 1,100 km would yield a subduction initiation timing of 43 Ma during actual extension in the Granada Basin, which seems unlikely since forced subduction initiation should correspond to localized compression (e.g., Lallemand & Arcay, 2021). Typically, backarc spreading follows, and may be caused by subduction initiation (Gurnis et al., 2004).

Overall, our projected timing of Farallon onset, slab penetration, reorganization, and LA initiation agrees with geological constraints across the Caribbean realm including:

1. Hypothesized proto-Farallon volcanic arc formation between 72 and 73 Ma (Buchs et al., 2010, 2011; Wegner et al., 2011);
2. Indications of the plate reorganization in the latest Paleocene, as constrained by the sedimentary record in western Cuba (e.g., Bralower & Iturralde-Vinent, 1997; Gordon et al., 1997; Meyerhoff & Hatten, 1968; Pardo, 1975);
3. The onset of rifting in the Yucatan basin (Rosencrantz, 1990);
4. The onset of Cayman spreading (~49 Ma Leroy et al., 2000);
5. Early to middle Eocene extension in the Granada basin (Aitken et al., 2011; Garroq et al., 2021), and
6. The GAC and LA magmatic records (Figure 3).

However, as with all such analyses, uncertainties arise from irregular resolution of tomography and plate thickness assumptions as well as complexities in terms of the mapping between seismic velocity anomalies and temperature. Among the complexities of mapping inferred slab structure is that diffusion will broaden thermal anomalies over time. However, as shown in Tan et al. (2002), for example, we expect convection of slabs to be advection-dominated on the timescales typical for the descent of a slab into the lower mantle. We therefore attribute the observed broadening of tomographic anomalies instead to reduced sinking velocities in the higher viscosity lower mantle or potential slab folding (e.g., Ribe et al., 2007).

Our profile was deemed most appropriate to capture the fullest extent of LA and Farallon subduction as it is sub-perpendicular to the reconstructed trenches and sub-parallel to the trajectory of subducted Farallon and Atlantic lithosphere (Figure 2a). However, if the profile cuts across the slabs obliquely, we would be measuring the apparent, rather than true thickness of the slab, leading to a slight overestimation of the total area of the subducted slab. Without well constrained knowledge of the slab architecture and how it has changed through time, it is difficult to ascertain whether the chosen profile truly crosses the slabs perpendicularly at depth.

Deviations in total subduction estimates, within reasonable uncertainties of geological constraints, should still preserve the relationship between Farallon slab anchoring and LA subduction onset, though would increase the time between the two events. As demonstrated in Figures S2 and S3 in Supporting Information S1, the modeled delay between anchoring and subduction initiation can vary by tens of Myrs depending on the density of the CLIP and strength of the weak zone. For both the Farallon and Atlantic slabs, we assume that subducted material associated with Mesozoic Farallon and Cretaceous to Paleocene GAC subduction histories are not included in our analysis.

According to previous reconstructions (Boschman et al., 2014; Pindell & Kennan, 2009), Farallon subduction occurred for \sim 200 Myrs prior to CLIP formation, the polarity reversal, and subduction beneath the CLIP. However, as discussed in Faccenna et al. (2017), an anomaly associated with Mesozoic subduction is not clear in tomography. Numerical models (Riel et al., 2023) show that the associated material may be disconnected from the up-dip Farallon/Cocos slab and may now reside somewhere in the lower mantle beneath the Caribbean plate. In our cross section, this previously subducted material may correspond to the subtle, fast anomalies at $>1,200$ km beneath the Caribbean plate (Figures 1 and 4) (cf. Zhu et al., 2020). Without higher resolution tomography, it is unclear if this material links directly to Farallon subduction.

For the history of Atlantic subduction beneath the GAC, it remains unclear whether the former GAC slab and the current LA slab are coherent, which may lead to an overestimation of total subduction. However, this material likely resides beneath South America at depths >900 km and is therefore not captured in our profile (e.g., Braszus et al., 2021; van Benthem et al., 2013).

Lastly, concerning the GAC and LA magmatic records, there is a 9–15 Myr difference between the onset of subduction and volcanism. This range is reasonable, considering that, for subduction zones globally, initiation-volcanism offsets range from a few Myrs to 15 Myrs (Hu & Gurnis, 2020). For Farallon subduction, this delay would imply that subduction initiation began slightly earlier than the onset of arc volcanism between 72 and 73 Ma (Buchs et al., 2010, 2011; Wegner et al., 2011), perhaps as early as 88 Ma (Pindell & Kennan, 2009). This timing indicates total subduction length at the upper end of our estimate, better matching our thinner plate thickness assumptions, or lower δv_p anomaly selection.

4.3. Effects of Farallon Slab Anchoring Throughout the Americas

A process similar to our proposed Caribbean reorganization model has been described south of the Caribbean to explain the Andean Orogeny in the Central Andes and subduction initiation in the Scotia Sea. We further posit that slab anchoring also played a role in the Laramide Orogeny during subduction of the Farallon plate beneath North America. As shown in Figure 7, these episodes of orogenesis or subduction initiation may be part of a north to south progressive Farallon slab anchoring process from the Late Cretaceous to the Paleogene. To illustrate this hypothesis, we show schematic cross sections associated with each subduction zone in Figure 7c.

In the case of the Scotia Arc, Schellart et al. (2023) suggest that the penetration of the Farallon slab into the lower mantle led to horizontal upper plate compression across a narrow segment of continental lithosphere that bridged South America and Antarctica. In this model, subduction initiation occurred in the Late Cretaceous to the Paleogene along the boundary between the intervening continental lithosphere and the oceanic lithosphere

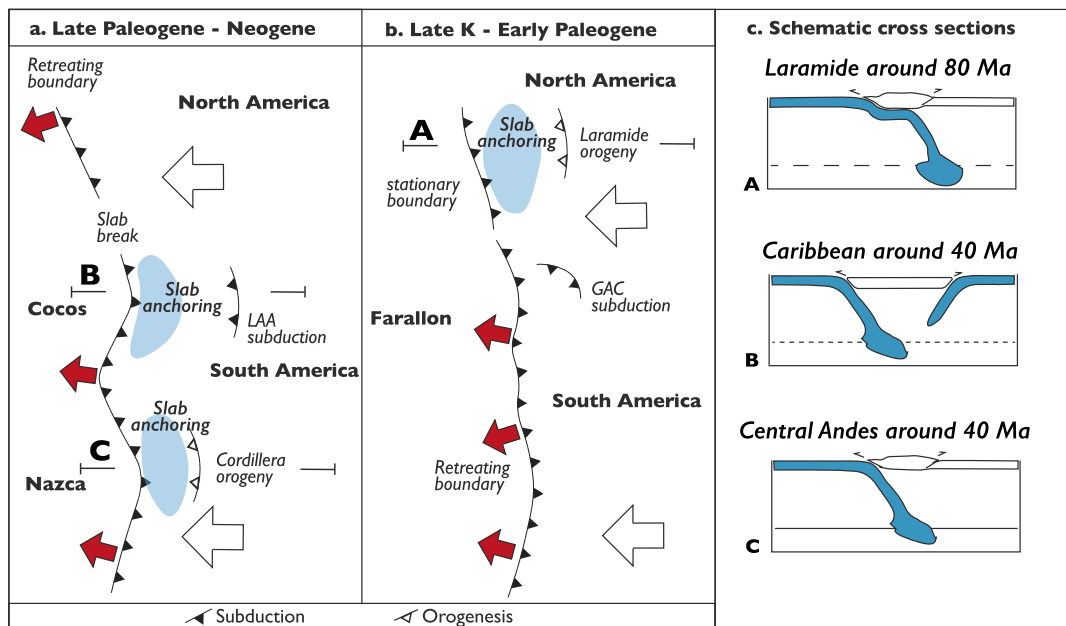


Figure 7. Progressive slab anchoring across the Americas. (a) Late Paleogene-Neogene compression in the Caribbean and Andes. (b) Late Cretaceous-Early Paleogene Laramide compression in North America. (c) Schematic cross sections illustrating the scenario for each segment of Farallon subduction. See text for discussion.

underlying the Weddell Sea to the east. However, unlike the Caribbean, subduction later ceased along the western margin of the Scotia plate with the formation of the Shackleton fracture zone in the Oligocene (e.g., van de Lagemaat et al., 2021) and the Farallon slab is not clearly evident in tomography beneath the Scotia plate. Due to these uncertainties, the Scotia subduction scenario is not included in Figure 7.

In the Central Andes, reconstructed motion of the trench through time suggests that the Farallon slab penetrated the lower mantle in the Eocene (Figures 7a–7c). This event resulted in a surge of compression and the initiation of the main phase of crustal thickening, leading to the formation of a bivariant orogeny and extensive underthrusting of the South American plate beneath the orogen (Faccenna et al., 2017). There is also evidence of slab penetration into the lower mantle and a compressional episode in the Eocene along the strike of the Farallon/Nazca/Cocos subduction zone between the Caribbean and the Central Andes. However, subsequent compression is limited, perhaps due to locally inefficient slab anchoring, shallow slab breakoff episodes, or a rigid upper plate.

Moving north along the Farallon subduction zone, episodes of significant compression occurred during the Laramide orogeny (Figures 7b and 7c). Current models propose a northeast younging of Laramide deformation and dynamic subsidence associated with the flat-subduction of the Hess Rise or Shatzky Rise conjugate (Humphreys et al., 2003; Liu et al., 2010; Livaccari et al., 1981; Tarduno et al., 1985). We suggest that slab shallowing and flattening were possible only if the slab tip was anchored into the lower mantle. During this stage, the trench is forced to migrate seaward due to the anchoring-induced change in basal tractions that allow the upper plate to move over the plateau (Espurt et al., 2008). A reduction in the net slab buoyancy by an incoming oceanic plateau, already largely supported by the viscous resistance of the strong lower mantle, could then induce a flat-slab episode. As shown by analog modeling (Espurt et al., 2008; Martinod et al., 2005), without slab anchoring, the upper plate would move “freely,” the trench would be fixed, and slab flattening is unlikely. We therefore suggest that this process is, like the onset of significant Andean shortening (Faccenna et al., 2017), also related to deep slab penetration.

Following the drift of North America, the position of the Farallon trench moved westward through time, aligning with the western edge of the deep high-velocity anomaly at ~80–90 Ma at 40° north. This coincides with the onset of shortening and surface deformation. The slowdown of trench retreat started roughly simultaneously. We infer that slab penetration into the lower mantle triggered the onset of shortening in the upper plate. In other words, the entrance of the slab into the lower mantle may have produced slab anchoring, slowing down its retrograde motion

and installing vigorous large-scale convection that may have dragged the upper plate against the trench (Becker & Faccenna, 2011; Faccenna et al., 2013; Yamato et al., 2013). The corresponding anchoring and flat slab geometry are shown in Figure 7c. In this case, the cessation of compression is related to a later episode of slab breakoff.

Overall, the Farallon slab diachronously penetrated the lower mantle from 50° north to 30° south, starting in the Late Cretaceous in the north and then propagating southward to Central and South America in the Eocene. However, effective slab anchoring is limited to specific portions of the slab—initially in the Laramide from 50° to 30° north, then in the Caribbean from 20° to 0° north, and finally in the Central Andes from 18° to 25° south. This localized anchoring manifested itself as a sinuous trench geometry and long-lived regional compressional episodes on the surface (Figure 7).

5. Conclusion

Plate reconstructions typically invoke the collision between the Caribbean plate and the Bahamas platform to explain the Paleogene reorganization of the Caribbean plate boundaries. However, this scenario is inconsistent with a range of geological and geophysical constraints. Based on the interpretation of seismic tomography, and guided by dynamic subduction models, we propose a new model to reconcile the observations. We suggest that the reorganization of the Caribbean can be linked to Farallon slab penetration into the lower mantle, which promotes the onset of subduction at the LA followed by punctuated eastward trench migration.

Slab penetration into the lower mantle can initiate subduction in the overriding plate if there is a region of pre-existing weakness, and that suture may be related to previous subduction during the Caribbean evolution from the Cretaceous to the Paleocene. Expanding beyond the Caribbean, slab penetration into the lower mantle could have affected most of the Late Cretaceous to recent subduction systems bordering the Americas. These effects include the North American Laramide orogeny during the Late Cretaceous, the onset of subduction in the LA during the Eocene, and the Cordilleran orogeny in South America during the Eocene.

Data Availability Statement

All files needed to run the ASPECT subduction models are contained within a permanent Zenodo repository (Conrad et al., 2024). Lesser Antilles magmatic data is downloadable on the EarthChem portal (<http://portal.earthchem.org>) using the bounding box tool and submitting individual queries using “Mineral” and “Whole Rock/Rock” for the selected material. A curated data set for the Greater Antilles is accessible in the form of a United States Geological Survey Open File Report (Wilson et al., 2019). GPlates and the Müller et al. (2019) reconstruction are downloadable on the EarthByte website (www.earthbyte.org).

Acknowledgments

We thank Serge Lallemand for insightful discussions during the early drafting of this manuscript. Several figures use the Generic Mapping tools of Wessel et al. (2019) for plotting, and Pál is dearly missed. Computational resources were provided by NSF ACCESS under allocation EAR-180026 to AFH. EC and TWB were partially supported by NSF EAR-1925939 and 1853856. We would also like to thank the editor, Jacqueline Dixon, for handling the manuscript and Nestor Cerpa and an additional anonymous reviewer for constructive reviews that helped to improve the manuscript from its original version.

References

Aitken, T., Mann, P., Escalona, A., & Christeson, G. L. (2011). Evolution of the Grenada and Tobago basins and implications for arc migration. *Marine and Petroleum Geology*, 28(1), 235–258. <https://doi.org/10.1016/j.marpetgeo.2009.10.003>

Allen, R., Collier, J., Stewart, A., Henstock, T., Goes, S., Rietbroek, A., & the VoiLA Team. (2019). The role of arc migration in the development of the Lesser Antilles: A new tectonic model for the Cenozoic evolution of the eastern Caribbean. *Geology*, 47(9), 891–895. <https://doi.org/10.1130/g46708.1>

Amaru, M. L. (2007). Global travel time tomography with 3-D reference models. *Geologica Ultraiectina*, 274, 174.

Baes, M., Sobolev, S. V., & Quinteros, J. (2018). Subduction initiation in mid-ocean induced by mantle suction flow. *Geophysical Journal International*, 215(3), 1515–1522. <https://doi.org/10.1093/gji/ggy335>

Bangerth, W., Dannberg, J., Gassmöller, R., Heister, T., Myhill, R., & Naliboff, J. (2023). Aspect: Advanced solver for problems in Earth’s convection, user manual. Zenodo. <https://doi.org/10.5281/zenodo>

Becker, T. W., & Faccenna, C. (2011). Mantle conveyor beneath the Tethyan collisional belt. *Earth and Planetary Science Letters*, 310(3–4), 453–461. <https://doi.org/10.1016/j.epsl.2011.08.021>

Becker, T. W., Lebedev, S., & Long, M. D. (2012). On the relationship between azimuthal anisotropy from shear wave splitting and surface wave tomography. *Journal of Geophysical Research Solid Earth*, 117(B1), B01306. <https://doi.org/10.1029/2011jb008705>

Becker, T. W., Schaeffer, A. J., Lebedev, S., & Conrad, C. P. (2015). Toward a generalized plate motion reference frame. *Geophysical Research Letters*, 42(9), 3188–3196. <https://doi.org/10.1002/2015GL063695>

Bellas, A., & Zhong, S. (2021). Seismic strain rate and flexure at the Hawaiian islands constrain the frictional coefficient. *Geochemistry, Geophysics, Geosystems*, 22(4), e2020GC009547. <https://doi.org/10.1029/2020gc009547>

Benford, B., DeMets, C., & Calais, E. (2012). GPS estimates of microplate motions, northern Caribbean: Evidence for a Hispaniola microplate and implications for earthquake hazard. *Geophysical Journal International*, 191(2), 481–490. <https://doi.org/10.1111/j.1365-246X.2012.05662.x>

Bird, D. E., Hall, S. A., Casey, J. F., & Millegan, P. S. (1999). Tectonic evolution of the Grenada basin. In *Sedimentary basins of the world* (Vol. 4, pp. 389–416). Elsevier. [https://doi.org/10.1016/s1874-5997\(99\)80049-5](https://doi.org/10.1016/s1874-5997(99)80049-5)

Blewitt, G., Kreemer, C., Hammond, W. C., & Gazeaux, J. (2016). MIDAS robust trend estimator for accurate GPS station velocities without step detection. *Journal of Geophysical Research Solid Earth*, 121(3), 2054–2068. <https://doi.org/10.1002/2015JB012552>

Boschman, L. M., van Hinsbergen, D. J., Torsvik, T. H., Spakman, W., & Pindell, J. L. (2014). Kinematic reconstruction of the Caribbean region since the Early Jurassic. *Earth-Science Reviews*, 138, 102–136. <https://doi.org/10.1016/j.earscirev.2014.08.007>

Bouysse, P. (1988). Opening of the Grenada back-arc basin and evolution of the Caribbean plate during the Mesozoic and early paleogene. *Tectonophysics*, 149(1–2), 121–143. [https://doi.org/10.1016/0040-1951\(88\)90122-9](https://doi.org/10.1016/0040-1951(88)90122-9)

Bouysse, P., & Guennoc, P. (1983). Donnees sur la structure de l'arc insulaire des petites antilles, entre ste-lucie et anguilla. *Marine Geology*, 53(1–2), 131–166. [https://doi.org/10.1016/0025-3227\(83\)90038-5](https://doi.org/10.1016/0025-3227(83)90038-5)

Bralower, T. J., & Iturralde-Vinent, M. A. (1997). Micropaleontological dating of the collision between the North American Plate and the Greater Antilles Arc in western Cuba. *PALAIOS*, 12(2), 133–150. <https://doi.org/10.2307/3515303>

Brandes, C., & Winsemann, J. (2018). From incipient island arc to doubly-vergent orogen: A review of geodynamic models and sedimentary basin-fills of southern Central America. *Island Arc*, 27(5), e12255. <https://doi.org/10.1111/iar.12255>

Braszus, B., Goes, S., Allen, R., Rietbroek, A., Collier, J., Harmon, N., et al. (2021). Subduction history of the Caribbean from upper-mantle seismic imaging and plate reconstruction. *Nature Communications*, 12(1), 4211. <https://doi.org/10.1038/s41467-021-24413-0>

Buchs, D. M., Arculus, R. J., Baumgartner, P. O., Baumgartner-Mora, C., & Ulianov, A. (2010). Late Cretaceous arc development on the SW margin of the Caribbean plate: Insights from the Golfito, Costa Rica, and Azuero, Panama, complexes. *Geochemistry, Geophysics, Geosystems*, 11(7), Q07S24. <https://doi.org/10.1029/2009GC002901>

Buchs, D. M., Baumgartner, P. O., Baumgartner-Mora, C., Flores, K., & Bandini, A. N. (2011). Upper cretaceous to miocene tectonostratigraphy of the azuero area (Panama) and the discontinuous accretion and subduction erosion along the middle American margin. *Tectonophysics*, 512(1–4), 31–46. <https://doi.org/10.1016/j.tecto.2011.09.010>

Burke, K. (1988). Tectonic evolution of the Caribbean. *Annual Review of Earth and Planetary Sciences*, 16(1), 201–230. <https://doi.org/10.1146/annurev.ea.16.050188.001221>

Calais, E., Symithe, S., Mercier de Lépinay, B., & Prépetit, C. (2016). Plate boundary segmentation in the northeastern Caribbean from geodetic measurements and Neogene geological observations. *Comptes Rendus Géoscience*, 348(1), 42–51. <https://doi.org/10.1016/j.crte.2015.10.007>

Castos, E., & Sorensen, S. (2003). Phengite-based chronology of K-and Ba-rich fluid flow in two paleosubduction zones. *Science*, 299(5603), 92–95. <https://doi.org/10.1126/science.1076977>

Cerpa, N. G., Hassani, R., Arcay, D., Lallemand, S., Garroq, C., Philippon, M., et al. (2021). Caribbean plate boundaries Control on the tectonic duality in the back-arc of the Lesser Antilles subduction zone during the Eocene. *Tectonophysics*, 40(11), e2021TC006885. <https://doi.org/10.1029/2021TC006885>

Chen, Y.-W., Wu, J., & Goes, S. (2024). Lesser Antilles slab reconstruction reveals lateral slab transport under the Caribbean since 50 Ma. *Earth and Planetary Science Letters*, 627, 118561. <https://doi.org/10.1016/j.epsl.2023.118561>

Christeson, G. L., Mann, P., Escalona, A., & Aitken, T. J. (2008). Crustal structure of the Caribbean–northeastern South America arc-continent collision zone. *Journal of Geophysical Research*, 113(B8), 1–19. <https://doi.org/10.1029/2007jb005373>

Conrad, E., Faccenna, C., Holt, A., & Becker, T. W. (2024). *Tectonic reorganization of the Caribbean plate system in the Paleogene driven by slab interactions and mantle convection*. Zenodo. <https://doi.org/10.5281/zenodo.11303715>

Cornée, J.-J., Boudagher-Fadel, M., Philippon, M., Léticée, J. L., Legendre, L., Maincent, G., et al. (2020). Paleogene carbonate systems of Saint Barthélemy, Lesser Antilles: Stratigraphy and general organization. *Newsletters on Stratigraphy*, 53(4), 461–478. <https://doi.org/10.1127/nos/2020/0587>

Corsini, M., Lardeaux, J., Verati, C., Voitus, E., & Balagne, M. (2011). Discovery of lower cretaceous symmetamorphic thrust tectonics in French Lesser Antilles (La Désirade Island, Guadeloupe): Implications for Caribbean geodynamics. *Tectonics*, 30(4), TC4005. <https://doi.org/10.1029/2011tc002875>

Cramer, F., Magni, V., Domeier, M., Shephard, G. E., Chotalia, K., Cooper, G., et al. (2020). A transdisciplinary and community-driven database to unravel subduction zone initiation. *Nature Communications*, 11(1), 3750. <https://doi.org/10.1038/s41467-020-1752-9>

DeMets, C., Gordon, R. G., & Argus, D. F. (2010). Geologically current plate motions. *Geophysical Journal International*, 181(1), 1–80. <https://doi.org/10.1111/j.1365-246X.2009.04491.x>

de Zoeten, R., & Mann, P. (1991). Structural geology and cenozoic tectonic history of the central Cordillera Septentrional, Dominican Republic. In *Geologic and tectonic development of the North America-Caribbean plate boundary in Hispaniola* (pp. 265–279). Geological Society of America. <https://doi.org/10.1130/SPE262-p217>

Dolan, J. F., Mullins, H. T., & Wald, D. J. (1998). Active tectonics of the north-central Caribbean: Oblique collision, strain partitioning, and opposing subducted slabs. In *Active strike-slip and collisional tectonics of the Northern Caribbean plate boundary zone* (pp. 1–61). Geological Society of America. <https://doi.org/10.1130/0-8137-2326-4.1>

Engdahl, E. R., van der Hilst, R. D., & Buland, R. (1998). Global teleseismic earthquake relocation with improved travel times and procedures for depth determination. *Bulletin of the Seismological Society of America*, 88(3), 722–743. <https://doi.org/10.1785/bssa0880030722>

Enns, A., Becker, T. W., & Schmeling, H. (2005). The dynamics of subduction and trench migration for viscosity stratification. *Geophysical Journal International*, 160(2), 761–775. <https://doi.org/10.1111/j.1365-246X.2005.02519.x>

Escalona, A., & Mann, P. (2011). Tectonics, basin subsidence mechanisms, and paleogeography of the Caribbean-South American plate boundary zone. *Marine and Petroleum Geology*, 28(1), 8–39. <https://doi.org/10.1016/j.marpetgeo.2010.01.016>

Escalona, A., Norton, I. O., Lawver, L. A., & Gahagan, L. (2021). Quantitative Plate tectonic reconstructions of the Caribbean region from Jurassic to present. In C. Bartolini (Ed.), *Memoir 123: South America-Caribbean-Central Atlantic plate boundary: Tectonic evolution, basin architecture, and Petroleum systems* (pp. 239–263). AAPG. <https://doi.org/10.1306/13692247M1233849>

Escuder Viruete, J., & Pérez Estaún, A. (2004). Trayectoria metamórfica pt relacionada con subducción en eclogitas del complejo de basamento de Samaná, Cordillera Septentrional, República Dominicana. *Geotemas*, 6, 37–40.

Escuder Viruete, J., Suárez-Rodríguez, A., Gabites, J., & Pérez-Estaún, A. (2015). The Imbert formation of northern Hispaniola: A tectono-sedimentary record of arc-continent collision and ophiolite emplacement in the northern Caribbean subduction-accretionary prism. *Solid Earth Discussions*, 7(2), 1827–1876. <https://doi.org/10.5194/sed-7-1827-2015>

Espurt, N., Funiciello, F., Martinod, J., Guillaume, B., Regard, V., Faccenna, C., & Brusset, S. (2008). Flat subduction dynamics and deformation of the South American plate: Insights from analog modeling. *Tectonophysics*, 473(1–2), 1–19. <https://doi.org/10.1029/2007TC002175>

Faccenna, C., Becker, T., Holt, A., & Brun, J. (2021). Mountain building, mantle convection, and supercontinents: Revisited. *Earth and Planetary Science Letters*, 564, 116905. <https://doi.org/10.1016/j.epsl.2021.116905>

Faccenna, C., Becker, T. W., Conrad, C. P., & Husson, L. (2013). Mountain building and mantle dynamics. *Tectonophysics*, 521, 80–93. <https://doi.org/10.1029/2012TC003176>

Faccenna, C., Giardini, D., Davy, P., & Argentieri, A. (1999). Initiation of subduction at Atlantic-type margins: Insights from laboratory experiments. *Journal of Geophysical Research Solid Earth*, 104(B2), 2749–2766. <https://doi.org/10.1029/1998JB900072>

Faccenna, C., Oncken, O., Holt, A. F., & Becker, T. W. (2017). Initiation of the Andean orogeny by lower mantle subduction. *Earth and Planetary Science Letters*, 463, 189–201. <https://doi.org/10.1016/j.epsl.2017.01.041>

Forsyth, D. W., & Uyeda, S. (1975). On the relative importance of the driving forces of plate motion. *Geophysical Journal of the Royal Astronomical Society*, 43(1), 163–200. <https://doi.org/10.1111/j.1365-246x.1975.tb00631.x>

Fox, P. J., Schreiber, E., & Heezen, B. C. (1971). The geology of the Caribbean crust: Tertiary sediments, granitic and basic rocks from the Aves Ridge. *Tectonophysics*, 12(2), 89–109. [https://doi.org/10.1016/0040-1951\(71\)90011-4](https://doi.org/10.1016/0040-1951(71)90011-4)

Fuchs, L., & Becker, T. W. (2019). Role of strain-dependent weakening memory on the style of mantle convection and plate boundary stability. *Geophysical Journal International*, 218(1), 601–618. <https://doi.org/10.1093/gji/ggz167>

Garcia, E. S. M., Sandwell, D. T., & Bassett, D. (2019). Outer trench slope flexure and faulting at Pacific basin subduction zones. *Geophysical Journal International*, 218(1), 708–728. <https://doi.org/10.1093/gji/ggz155>

García-Casco, A., Iturralde-Vinent, M. A., & Pindell, J. (2008). Latest Cretaceous collision/accretion between the Caribbean plate and Caribean: Origin of metamorphic Terranes in the Greater Antilles. *International Geology Review*, 50(9), 781–809. <https://doi.org/10.2747/0020-6814.50.9.781>

Garrocq, C., Lallemand, S., Marcaillou, B., Lebrun, J.-F., Padron, C., Klingelhoefer, F., et al. (2021). Genetic relations between the Aves Ridge and the Grenada back-arc basin, east Caribbean sea. *Journal of Geophysical Research Solid Earth*, 126(2), e2020JB020466. <https://doi.org/10.1029/2020jb020466>

Gordon, M. B., Mann, P., Cáceres, D., & Flores, R. (1997). Cenozoic tectonic history of the North America-Caribbean plate boundary zone in western Cuba. *Journal of Geophysical Research Solid Earth*, 102(B5), 10055–10082. <https://doi.org/10.1029/96JB03177>

Granja Bruña, J., Carbó-Gorosabel, A., Llanes Estrada, P., Muñoz-Martín, A., ten Brink, U., Gómez Ballesteros, M., et al. (2014). Morphotecture at the junction between the Beata ridge and the Greater Antilles island arc (offshore Hispaniola southern slope). *Tectonophysics*, 618, 138–163. <https://doi.org/10.1016/j.tecto.2014.02.001>

Gurnis, M. (1992). Rapid continental subsidence following the initiation and evolution of subduction. *Science*, 255(5051), 1556–1558. <https://doi.org/10.1126/science.255.5051.1556>

Gurnis, M., Hall, C., & Lavier, L. (2004). Evolving force balance during incipient subduction. *Geochemistry, Geophysics, Geosystems*, 5(7), 453. <https://doi.org/10.1029/2003gc000681>

Hafkenscheid, E., Wortel, M. J. R., & Spakman, W. (2006). Subduction history of the Tethyan region derived from seismic tomography and tectonic reconstructions. *Journal of Geophysical Research Solid Earth*, 111, B08401. <https://doi.org/10.1029/2005JB003791>

Hager, B. H. (1984). Subducted slabs and the geoid: Constraints on mantle rheology and flow. *Journal of Geophysical Research Solid Earth*, 89(B7), 6003–6015. <https://doi.org/10.1029/jb089ib07p06003>

Hager, B. H., & O'Connell, R. J. (1978). Subduction zone dip angles and flow derived by plate motion. *Tectonophysics*, 50(2–3), 111–133. [https://doi.org/10.1016/0040-1951\(78\)90130-0](https://doi.org/10.1016/0040-1951(78)90130-0)

Hall, R., & Spakman, W. (2015). Mantle structure and tectonic history of SE Asia. *Tectonophysics*, 658, 14–45. <https://doi.org/10.1016/j.tecto.2015.07.003>

Harris, C. W., Miller, M. S., & Porritt, R. W. (2018). Tomographic imaging of slab segmentation and deformation in the Greater Antilles. *Geochemistry, Geophysics, Geosystems*, 19(8), 2292–2307. <https://doi.org/10.1029/2018GC007603>

Heister, T., Dannberg, J., Gassmöller, R., & Bangerth, W. (2017). High accuracy mantle convection simulation through modern numerical methods. II: Realistic models and problems. *Geophysical Journal International*, 210(2), 833–851. <https://doi.org/10.1093/gji/ggx195>

Heubeck, C., Mann, P., Dolan, J., & Monechi, S. (1991). Diachronous uplift and recycling of sedimentary basins during Cenozoic tectonic transgression, northeastern Caribbean plate margin. *Sedimentary Geology*, 70(1), 1–32. [https://doi.org/10.1016/0037-0738\(91\)90063-J](https://doi.org/10.1016/0037-0738(91)90063-J)

Heuret, A., & Lallemand, S. (2005). Plate motions, slab dynamics and back-arc deformation. *Physics of the Earth and Planetary Interiors*, 149(1), 31–51. <https://doi.org/10.1016/j.pepi.2004.08.022>

Hirth, G., & Kohlstedt, D. (2003). Rheology of the upper mantle and the mantle wedge: A view from the experimentalists. *Geophysical Monograph-American Geophysical Union*, 138, 83–106.

Holt, A. F., & Condit, C. B. (2021). Slab temperature evolution over the lifetime of a subduction zone. *Geochemistry, Geophysics, Geosystems*, 22(6), e2020GC009476. <https://doi.org/10.1029/2020GC009476>

Holt, A. F., Royden, L. H., & Becker, T. W. (2017). The dynamics of double slab subduction. *Geophysical Journal International*, 209, 250–265.

Hu, J., & Gurnis, M. (2020). Subduction duration and slab dip. *Geochemistry, Geophysics, Geosystems*, 21(4), e2019GC008862. <https://doi.org/10.1029/2019GC008862>

Huerta, P. H., & Pérez-Estaún, A. (2002). Estructura del cinturón de pliegues y cabalgamientos de Peralta, República Dominicana. *Acta Geologica Hispanica*, 183–205.

Humphreys, E., Hessler, E., Dueker, K., Farmer, G. L., Erslev, E., & Atwater, T. (2003). How Laramide-age hydration of North American lithosphere by the Farallon slab controlled subsequent activity in the western United States. *International Geology Review*, 45(7), 575–595. <https://doi.org/10.2747/0020-6814.45.7.575>

Husson, L., Guillaume, B., Funicello, F., Faccenna, C., & Royden, L. H. (2012). Unraveling topography around subduction zones from laboratory models. *Tectonophysics*, 526–529, 5–15. <https://doi.org/10.1016/j.tecto.2011.09.001>

Iturralde-Vinent, M. A. (1994). Cuban geology: A new plate-tectonic synthesis. *Journal of Petroleum Geology*, 17(1), 39–69. <https://doi.org/10.1111/j.1747-5457.1994.tb00113.x>

Iturralde-Vinent, M. A., & MacPhee, R. D. (1999). Paleogeography of the Caribbean region: Implications for Cenozoic biogeography. In *Bulletin of the AMNH: No. 238*.

Iturralde-Vinent, M. A., & MacPhee, R. D. (2023). New evidence for late Eocene-early Oligocene uplift of Aves Ridge and paleogeography of GAARlania. *Geológica Acta*, 21, 1–10. <https://doi.org/10.1344/geologicaacta2023.21.5>

Jolly, W. T., Lidiak, E. G., Schellekens, J. H., & Santos, H. (1998). Volcanism, tectonics, and stratigraphic correlations in Puerto Rico. In *Tectonics and geochemistry of the northeastern Caribbean* (pp. 1–34). Geological Society of America. <https://doi.org/10.1130/0-8137-2322-1.1>

Joyce, J. (1991). Blueschist metamorphism and deformation on the Samana Peninsula; a record of subduction and collision in the Greater Antilles. In *Geologic and tectonic development of the North America-Caribbean plate boundary in Hispaniola*. Geological Society of America special Paper (Vol. 262, pp. 47–76). <https://doi.org/10.1130/spe262-p47>

Kamenov, G. D., Perfit, M. R., Lewis, J. F., Goss, A. R., Arévalo, R., & Shuster, R. D. (2011). Ancient lithospheric source for Quaternary lavas in Hispaniola. *Nature Geoscience*, 4(8), 554–557. <https://doi.org/10.1038/ngeo1203>

Karato, S.-I., & Wu, P. (1993). Rheology of the upper mantle: A synthesis. *Science*, 260(5109), 771–778. <https://doi.org/10.1126/science.260.5109.771>

Kesler, S. E., Sutter, J. F., Barton, J. M., & Speck, R. C. (1991). Age of intrusive rocks in northern Hispaniola. In P. Mann, G. Draper, & J. F. Lewis (Eds.), *Geologic and tectonic development of the North America-Caribbean plate boundary in Hispaniola* (Vol. 262, pp. 165–172). Geological Society of America. <https://doi.org/10.1130/SPE262-p165>

Kolarsky, R. A., Mann, P., Monechi, S., Mann, P., Meyerhoff-Hull, D., & Pessagno, E. A. (1995). Stratigraphic development of southwestern Panama as determined from integration of marine seismic data and onshore geology. In *Geological Society of America special papers* (Vol. 295, pp. 159–200). Geological Society of America. <https://doi.org/10.1130/SPE295-p159>

Kronbichler, M., Heister, T., & Bangerth, W. (2012). High accuracy mantle convection simulation through modern numerical methods. *Geophysical Journal International*, 191(1), 12–29. <https://doi.org/10.1111/j.1365-246X.2012.05609.x>

Lallemand, S., & Arcay, D. (2021). Subduction initiation from the earliest stages to self-sustained subduction: Insights from the analysis of 70 Cenozoic sites. *Earth-Science Reviews*, 221, 103779. <https://doi.org/10.1016/j.earscirev.2021.103779>

Laó-Dávila, D. A. (2014). Collisional zones in Puerto Rico and the northern Caribbean. *Journal of South American Earth Sciences*, 54, 1–19. <https://doi.org/10.1016/j.jsames.2014.04.009>

Legendre, L., Philippin, M., Münch, P., Leteice, J.-L., Noury, M., Maincent, G., et al. (2018). Trench bending initiation: Upper plate strain pattern and volcanism. Insights from the Lesser Antilles arc, St. Barthelemy island, French West Indies. *Tectonics*, 37(9), 2777–2797. <https://doi.org/10.1029/2017tc004921>

Leroy, S., Mauffret, A., Patriat, P., & Mercier de Lepinay, B. (2000). An alternative interpretation of the Cayman trough evolution from a re-identification of magnetic anomalies. *Geophysical Journal International*, 141(3), 539–557. <https://doi.org/10.1046/j.1365-246x.2000.00059.x>

Lewis, J. F., Amarante, A., Bloise, G., Jiménez, G. J. G., & Dominguez, H. D. (1991). Lithology and stratigraphy of upper Cretaceous volcanic and volcanioclastic rocks of the Tireo Group, Dominican Republic and correlations with the Massif du Nord in Haiti. In *Geologic and tectonic development of the North America-Caribbean plate boundary in Hispaniola* (pp. 115–141). Geological Society of America. <https://doi.org/10.1130/SPE262-p143>

Li, Y., & Gurnis, M. (2023). A simple force balance model of subduction initiation. *Geophysical Journal International*, 232(1), 128–146. <https://doi.org/10.1093/gji/ggac332>

Lidiak, E. G., & Anderson, T. H. (2015). Evolution of the Caribbean plate and origin of the Gulf of Mexico in light of plate motions accommodated by strike-slip faulting. In *Late Jurassic margin of Laurasia—A record of faulting* (Vol. 513, pp. 1–88). [https://doi.org/10.1130/2015.2513\(01](https://doi.org/10.1130/2015.2513(01)

Liu, L., Gurnis, M., Seton, M., Saleby, J., Müller, R. D., & Jackson, J. M. (2010). The role of oceanic plateau subduction in the Laramide orogeny. *Nature Geoscience*, 3(5), 353–357. <https://doi.org/10.1038/ngeo829>

Livaccari, R. F., Burke, K., & Şengör, A. M. C. (1981). Was the Laramide orogeny related to subduction of an oceanic plateau? *Nature*, 289(5795), 276–278. <https://doi.org/10.1038/289276a0>

Mann, P., & Burke, K. (1984). Neotectonics of the Caribbean. *Reviews of Geophysics*, 22(4), 309–362. <https://doi.org/10.1029/rg022i004p00309>

Mann, P., Calais, E., Ruegg, J.-C., DeMets, C., Jansma, P. E., & Mattioli, G. S. (2002). Oblique collision in the northeastern Caribbean from GPS measurements and geological observations. *Tectonophysics*, 371(6), 7–17–26. <https://doi.org/10.1029/2001TC001304>

Mann, P., Draper, G., & Lewis, J. F. (1991). An overview of the geologic and tectonic development of Hispaniola. In *Geologic and tectonic development of the North America-Caribbean plate boundary in Hispaniola* (pp. 1–28). Geological Society of America. <https://doi.org/10.1130/SPE262-p1>

Mann, P., Taylor, F. W., Edwards, R. L., & Ku, T.-L. (1995). Actively evolving microplate formation by oblique collision and sideways motion along strike-slip faults: An example from the northeastern Caribbean plate margin. *Tectonophysics*, 246(1), 1–69. [https://doi.org/10.1016/0040-1951\(94\)00268-E](https://doi.org/10.1016/0040-1951(94)00268-E)

Martinod, J., Funiciello, F., Faccenna, C., Labanieh, S., & Regard, V. (2005). Dynamical effects of subducting ridges: Insights from 3-D laboratory models. *Geophysical Journal International*, 163(3), 1137–1150. <https://doi.org/10.1111/j.1365-246x.2005.02797.x>

Mauffret, A., & Leroy, S. (1997). Seismic stratigraphy and structure of the Caribbean igneous province. *Tectonophysics*, 283(1–4), 61–104. [https://doi.org/10.1016/s0040-1951\(97\)00103-0](https://doi.org/10.1016/s0040-1951(97)00103-0)

Meyerhoff, A., & Hatten, C. (1968). Diapiric structures in central Cuba. In *M 8: Diapirism and diapirs* (pp. 315–357). AAPG Special Volumes.

Müller, M. S., & Becker, T. W. (2012). Mantle flow deflected by interactions between subducted slabs and cratonic keels. *Nature Geoscience*, 5(10), 726–730. <https://doi.org/10.1038/geo1553>

Montheil, L., Philippin, M., Münch, P., Camps, P., Vaes, B., Cornée, J.-J., et al. (2023). Paleomagnetic rotations in the northeastern Caribbean region reveal major intraplate deformation since the Eocene. *Tectonophysics*, 42(8), e2022TC007706. <https://doi.org/10.1029/2022TC007706>

Mora, J. A., Onccken, O., Le Breton, E., Ibáñez-Mejía, M., Faccenna, C., Veloza, G., et al. (2017). Linking Late Cretaceous to Eocene tectonostratigraphy of the San Jacinto fold belt of NW Colombia with Caribbean plateau collision and flat subduction. *Tectonics*, 36(11), 2599–2629. <https://doi.org/10.1029/2017tc004612>

Moresi, L. N., & Solomatov, V. S. (1998). Mantle convection with a brittle lithosphere: Thoughts on the global tectonic styles of the Earth and Venus. *Geophysical Journal International*, 133(3), 669–682. <https://doi.org/10.1046/j.1365-246x.1998.00521.x>

Mueller, S., & Phillips, R. J. (1991). On the initiation of subduction. *Journal of Geophysical Research Solid Earth*, 96(B1), 651–665. <https://doi.org/10.1029/90jb02237>

Müller, R. D., Cannon, J., Qin, X., Watson, R. J., Gurnis, M., Williams, S., et al. (2018). GPlates: Building a Virtual Earth through deep time. *Geochemistry, Geophysics, Geosystems*, 19(7), 2243–2261. <https://doi.org/10.1029/2018GC007584>

Müller, R. D., Zahirovic, S., Williams, S. E., Cannon, J., Seton, M., Bower, D. J., et al. (2019). A global plate model including lithospheric deformation along major rifts and orogens since the Triassic. *Tectonophysics*, 38(6), 1884–1907. <https://doi.org/10.1029/2018TC005462>

Neill, I., Gibbs, J. A., Hastie, A. R., & Kerr, A. C. (2010). Origin of the volcanic complexes of La Désirade, Lesser Antilles: Implications for tectonic reconstruction of the Late Jurassic to Cretaceous Pacific-proto Caribbean margin. *Lithos*, 120(3–4), 407–420. <https://doi.org/10.1016/j.lithos.2010.08.026>

Neill, I., Kerr, A. C., Hastie, A. R., Stanek, K.-P., & Millar, I. L. (2011). Origin of the Aves Ridge and Dutch–Venezuelan Antilles: Interaction of the cretaceous ‘Great Arc’ and Caribbean–Colombian oceanic plateau? *Journal of the Geological Society*, 168(2), 333–348. <https://doi.org/10.1144/0016-76492010-067>

Nikolaeva, K., Gerya, T. V., & Marques, F. O. (2010). Subduction initiation at passive margins: Numerical modeling. *Journal of Geophysical Research Solid Earth*, 115(B3), B03406. <https://doi.org/10.1029/2009JB006549>

Padron, C., Klingelhoefer, F., Marcaillou, B., Lebrun, J.-F., Lallemand, S., Garrocq, C., et al. (2021). Deep structure of the Grenada basin from wide-angle seismic, bathymetric and gravity data. *Journal of Geophysical Research: Solid Earth*, 126(2), e2020JB020472. <https://doi.org/10.1029/2020JB020472>

Pardo, G. (1975). Geology of Cuba. In A. E. M. Nairn & F. G. Stehli (Eds.), *The Gulf of Mexico and the Caribbean* (pp. 553–615). Springer US. https://doi.org/10.1007/978-1-4684-8535-6_13

Philippon, M., Cornée, J.-J., Münch, P., Van Hinsbergen, D. J., BouDagher-Fadel, M., Gailler, L., et al. (2020). Eocene intra-plate shortening responsible for the rise of a faunal pathway in the northeastern Caribbean realm. *PLoS One*, 15(10), e0241000. <https://doi.org/10.1371/journal.pone.0241000>

Phipps Morgan, J., Ranero, C., & Vannucchi, P. (2008). Intra-arc extension in Central America: Links between plate motions, tectonics, volcanism, and geochemistry. *Earth and Planetary Science Letters*, 272(1), 365–371. <https://doi.org/10.1016/j.epsl.2008.05.004>

Pindell, J. L., & Barrett, S. F. (1991). Geological evolution of the Caribbean region: A plate-tectonic perspective. In *Special paper of the geological society of America*. <https://doi.org/10.1130/DNAG-GNA-H.405>

Pindell, J. L., & Kennan, L. (2009). Tectonic evolution of the gulf of Mexico, caribbean and northern South America in the mantle reference frame: An update. *Geological Society, London, Special Publications*, 328(1), 1–55. <https://doi.org/10.1144/SP328.1>

Pindell, J. L., Kennan, L., Stanek, K. P., Maresch, W., & Draper, G. (2006). Foundations of gulf of Mexico and Caribbean evolution: Eight controversies resolved. *Geologica Acta: An International Earth Science Journal*, 4(1–2), 303–341.

Pubellier, M., Mauffret, A., Leroy, S., Vila, J. M., & Amilcar, H. (2000). Plate boundary readjustment in oblique convergence: Example of the Neogene of Hispaniola, Greater Antilles. *Tectonophysics*, 39(4), 630–648. <https://doi.org/10.1029/2000TC900007>

Pusok, A. E., & Stegman, D. R. (2019). Formation and stability of same-dip double subduction systems. *Journal of Geophysical Research Solid Earth*, 124(7), 7387–7412. <https://doi.org/10.1029/2018JB017027>

Ribe, N. M., Stutzmann, E., Ren, Y., & Van Der Hilst, R. (2007). Buckling instabilities of subducted lithosphere beneath the transition zone. *Earth and Planetary Science Letters*, 254(1–2), 173–179. <https://doi.org/10.1016/j.epsl.2006.11.028>

Riel, N., Duarte, J. C., Almeida, J., Kaus, B. J., Rosas, F., Rojas-Agramonte, Y., & Popov, A. (2023). Subduction initiation triggered the Caribbean large igneous province. *Nature Communications*, 14(1), 786. <https://doi.org/10.1038/s41467-023-36419-x>

Rojas-Agramonte, Y., Neubauer, F., Bojar, A. V., Hejl, E., Handler, R., & García-Delgado, D. E. (2006). Geology, age and tectonic evolution of the Sierra Maestra Mountains, southeastern Cuba. *Geologica Acta*.

Román, Y., Pujols, E., Cavosie, A., & Stockli, D. (2020). Timing and magnitude of progressive exhumation and deformation associated with Eocene arc-continent collision in the NE Caribbean plate. *Geological Society of America Bulletin*, 133(5–6), 1256–1266. <https://doi.org/10.1130/B35715.1>

Rosencrantz, E. (1990). Structure and tectonics of the Yucatan Basin, caribbean Sea, as determined from seismic reflection studies. *Tectonophysics*, 9(5), 1037–1059. <https://doi.org/10.1029/TC009h005p01037>

Sandiford, D., & Craig, T. J. (2023). Plate bending earthquakes and the strength distribution of the lithosphere. *Geophysical Journal International*, 235(1), 488–508. <https://doi.org/10.1093/gji/ggad230>

Schellart, W., Strak, V., Beniest, A., Duarte, J., & Rosas, F. (2023). Subduction invasion polarity switch from the pacific to the Atlantic ocean: A new geodynamic model of subduction initiation based on the scotia sea region. *Earth-Science Reviews*, 236, 104277. <https://doi.org/10.1016/j.earscirev.2022.104277>

Shipper, K., & Mann, P. (2024). Crustal structure, deformational history, and tectonic origin of the Bahamas carbonate platform. *Geochemistry, Geophysics, Geosystems*, 25(6), e2023GC011300. <https://doi.org/10.1029/2023gc011300>

Siravo, G., Fellin, M. G., Faccenna, C., Bayona, G., Lucci, F., Molin, P., & Maden, C. (2018). Constraints on the Cenozoic deformation of the northern eastern cordillera, Colombia. *Tectonics*, 37(11), 4311–4337. <https://doi.org/10.1029/2018tc005162>

Smith, A. L., Schellekens, J. H., & Díaz, A.-L. M. (1998). Batholiths as markers of tectonic change in the northeastern Caribbean. In *Tectonics and geochemistry of the northeastern Caribbean* (pp. 99–122). Geological Society of America. <https://doi.org/10.1130/0-8137-2322-1.99>

Stanek, K., Maresch, W., & Pindell, J. (2009). The geotectonic story of the northwestern branch of the Caribbean arc: Implications from structural and geochronological data of Cuba. *Geological Society, London, Special Publications*, 328(1), 361–398. <https://doi.org/10.1144/sp328.15>

Symithe, S., Calais, E., Chabalier, J. B. D., Robertson, R., & Higgins, M. (2015). Current block motions and strain accumulation on active faults in the Caribbean. *Journal of Geophysical Research Solid Earth*, 120(5), 3748–3774. <https://doi.org/10.1002/2014JB011779>

Tan, E., Gurnis, M., & Han, L. (2002). Slabs in the lower mantle and their modulation of plume formation. *Geochemistry, Geophysics, Geosystems*, 3(11), 1–24. <https://doi.org/10.1029/2001gc000238>

Tarduno, J. A., McWilliams, M., Debiche, M. G., Sliter, W. V., & Blake, M. C. (1985). Franciscan complex Calera limestones: Accreted remnants of Farallon Plate oceanic plateaus. *Nature*, 317(6035), 345–347. <https://doi.org/10.1038/317345a0>

Toth, J., & Gurnis, M. (1998). Dynamics of subduction initiation at preexisting fault zones. *Journal of Geophysical Research*, 103(B8), 18053–18067. <https://doi.org/10.1029/98jb01076>

van Benthem, S., Govers, R., Spakman, W., & Wortel, R. (2013). Tectonic evolution and mantle structure of the Caribbean. *Journal of Geophysical Research Solid Earth*, 118(6), 3019–3036. <https://doi.org/10.1002/jgrb.50235>

van Benthem, S., Govers, R., & Wortel, R. (2014). What drives microplate motion and deformation in the northeastern Caribbean plate boundary region? *Tectonophysics*, 33(5), 850–873. <https://doi.org/10.1002/2013TC003402>

van de Lagemaat, S. H., Swart, M. L., Vaes, B., Kosters, M. E., Boschman, L. M., Burton-Johnson, A., et al. (2021). Subduction initiation in the scotia sea region and opening of the drake passage: When and why? *Earth-Science Reviews*, 215, 103551. <https://doi.org/10.1016/j.earscirev.2021.103551>

Wegner, W., Wörner, G., Harmon, R. S., & Jicha, B. R. (2011). Magmatic history and evolution of the central American Land Bridge in Panama since Cretaceous times. *Geological Society of America Bulletin*, 123(3–4), 703–724. <https://doi.org/10.1130/B30109.1>

Wessel, P., Luis, J. F., Uieda, L., Scharroo, R., Wobbe, F., Smith, W. H. F., & Tian, D. (2019). The generic mapping tools version 6. *Geochemistry, Geophysics, Geosystems*, 20(11), 5556–5564. <https://doi.org/10.1029/2019GC008515>

Whattam, S. A. (2018). Primitive magmas in the early Central American volcanic arc system generated by plume-induced subduction initiation. *Frontiers in Earth Science*, 6, 114. <https://doi.org/10.3389/feart.2018.00114>

Whattam, S. A., & Stern, R. J. (2015). Late Cretaceous plume-induced subduction initiation along the southern margin of the Caribbean and NW South America: The first documented example with implications for the onset of plate tectonics. *Gondwana Research*, 27(1), 38–63. <https://doi.org/10.1016/j.gr.2014.07.011>

Wilson, F. H., Orris, G., & Gray, F. (2019). *Preliminary geologic map of the Greater Antilles and the Virgin Islands (USGS numbered series no. 2019-1036)*. USGS. <https://doi.org/10.3133/of20191036>

Winsemann, J. (1992). *Tiefwasser-sedimentationsprozesse und-produkte in den forearc-becken des mittelamerikanischen inselbogensystems: Eine sequenzstratigraphische analyse*. Institut für Geologie und Paläontologie.

Wright, J. E., & Wyld, S. J. (2011). Late Cretaceous subduction initiation on the eastern margin of the Caribbean-Colombian Oceanic Plateau: One Great Arc of the Caribbean (?). *Geosphere*, 7(2), 468–493. <https://doi.org/10.1130/GES00577.1>

Yamato, P., Husson, L., Becker, T. W., & Pedoja, K. (2013). Passive margins getting squeezed in the mantle convection vice. *Tectonophysics*, 32(6), 1559–1570. <https://doi.org/10.1002/2013TC003375>

Yamato, P., Husson, L., Braun, J., Loiselet, C., & Thieulot, C. (2009). Influence of surrounding plates on 3D subduction dynamics. *Geophysical Research Letters*, 36(7), 1–5. <https://doi.org/10.1029/2008GL036942>

Yang, T., Gurnis, M., & Zahirovic, S. (2016). Mantle-induced subsidence and compression in SE Asia since the early Miocene. *Geophysical Research Letters*, 43(5), 1901–1909. <https://doi.org/10.1002/2016GL068050>

Yang, T., Gurnis, M., & Zahirovic, S. (2018). Slab avalanche-induced tectonics in self-consistent dynamic models. *Tectonophysics*, 746, 251–265. <https://doi.org/10.1016/j.tecto.2016.12.007>

Zhong, S., & Gurnis, M. (1995). Mantle convection with plates and Mobile, faulted Plate Margins. *Science*, 267(5199), 838–843. <https://doi.org/10.1126/science.267.5199.838>

Zhu, H., Stern, R. J., & Yang, J. (2020). Seismic evidence for subduction-induced mantle flows underneath middle America. *Nature Communications*, 11(1), 2075. <https://doi.org/10.1038/s41467-020-15492-6>